# On the Anharmonic XCN Bending Modes of the Quasilinear Molecules BrCNO and ClCNO

**Holger Lichau,[†,‡] Charles W. Gillies,[†,§] Jennifer Z. Gillies,[†,||] Stephen C. Ross,[⊥] Brenda P. Winnewisser,[†,#] and Manfred Winnewisser[†,#]**

*Physikalisch-Chemisches Institut, Justus-Liebig-Universität, D-35392 Gießen, Germany, and Department of Physics, University of New Brunswick, Fredericton, New Brunswick, Canada E3B 5A3*

*Received: May 31, 2001; In Final Form: August 27, 2001*

The millimeter-wave spectra of the unstable halofulminates BrCNO and ClCNO were recorded at room temperature in several frequency intervals between 52 and 230 GHz. Besides rotational transitions in the vibrational ground state, transitions in numerous thermally excited states of the XCN bending mode (X = Br or Cl) could be observed. The irregular sequence of these satellites indicated that in both molecules, the XCN bending mode is highly anharmonic. Indeed, the XCNO molecules exhibit truly quasilinear behavior. From semirigid bender analyses of the rotational data, the effective potential functions and their barriers to linearity were determined. The barrier heights were found to be 130.82 (56) $cm^{-1}$ for BrCNO and 166.86 (84) $cm^{-1}$ for ClCNO, resulting in quasilinearity parameters $\gamma_0$ of +0.362 and +0.416, respectively.

## Introduction

Although the concept of molecular quasilinearity was introduced four decades ago,[1] only a few characteristic examples of quasilinear molecules or quasisymmetric top molecules have been described in the spectroscopic literature.[2−5] Hence, the analysis of the unusual internal dynamics arising from a highly anharmonic bending potential function with a low barrier to linearity still remains a challenging task for spectroscopy.

Two successive studies utilizing low-resolution infrared and photoelectron spectroscopy in combination with various medium-level ab initio calculations had suggested that bromofulminate, BrCNO, and chlorofulminate, ClCNO, might possess highly anharmonic XCN bending modes (X = Br or Cl) and hence fall into the regime of pronounced quasilinearity.[6,7] We decided to examine this possibility by recording the rotational spectra of both molecules at room temperature in the millimeter-wave region. A preliminary analysis of the rotational spectrum of BrCNO in fact provided evidence for BrCNO being truly quasilinear, that is, roughly in the middle between the linear and the bent limiting case.[8] In the present paper, we give an account of the experimental methods used to obtain the rotational spectra of both molecules and present the analyses of these spectra. Effective bending potentials for the large-amplitude XCN bending motions of both molecules were obtained from these analyses. Stimulated by this work, Koput[9] has determined the structural parameters of both molecules and their XCN bending potential functions by employing high-level ab initio calculations using the CCSD(T) coupled-cluster method and basis sets of double- through quintuple-zeta quality. We can thus compare our experimental results with these state-of-the-art theoretical predictions.

## Experimental Procedures

The millimeter-wave spectrum of BrCNO was recorded in the frequency ranges of 52−148 and 159−179 GHz. The experimental setup included three different backward-wave oscillator (BWO) based synthesizers[10] from Analytische Messtechnik Chemnitz (AMC) together with Schottky-barrier diode detectors matched to each frequency band. In these synthesizers, the output frequency of the BWO is phase-locked to a harmonic of a reference frequency around 5 GHz. By modulating the reference frequency, frequency modulation can be applied to the phase-stabilized millimeter-wave radiation, allowing phase-sensitive detection of the absorption signal. In addition, a frequency doubler[11] and a liquid-helium-cooled InSb hot-electron detector were used to access the frequency range 210−230 GHz.

The chemical instability of BrCNO required a continuous flow through our 2.5 m long free-space glass cell. The sample molecules were generated directly at the inlet port by pyrolysis of gaseous dibromoformaldoxime $Br_2CNOH$.[6] At a mass flow rate of 10 mg/min, the total pressure in the absorption cell was maintained at approximately 0.8 Pa (6 mTorr). The pyrolysis was performed in a simple quartz tube with an inner diameter of 11 mm. For initial experiments, this tube was heated to 1070 K along a section of 20 cm, but later on, the heated zone was extended to 25 cm and the temperature reduced to 930 K, which resulted in a slightly higher yield of BrCNO.

Below 179 GHz, the modulation deviation was chosen to be 250 kHz to maximize signal strength, whereas above 210 GHz, the increasing Doppler width of the absorption lines required a larger modulation deviation of 400 kHz. Switching to the InSb detector for the higher frequency range limited the modulation

* To whom correspondence should be addressed. Manfred Winnewisser, Department of Physics, The Ohio State University, 174 West 18th Avenue, Columbus, OH 43210-1106. Phone: 614-688-8140. Fax: 614-292-7557. E-mail: Winnem@mps.ohio-state.edu.

† Justus-Liebig-Universität.

‡ Current address: Department of Chemistry, Princeton University, Princeton, NJ 08544.

§ Permanent address: Department of Chemistry, Rensselaer Polytechnic Institute, Troy, NY 12180.

|| Permanent address: Department of Chemistry, Siena College, Loudonville, NY 12211.

⊥ University of New Brunswick.

# Current address: Department of Physics, The Ohio State University, Columbus, OH 43210.

10.1021/jp012067u CCC: $20.00 
Published on Web 10/16/2001

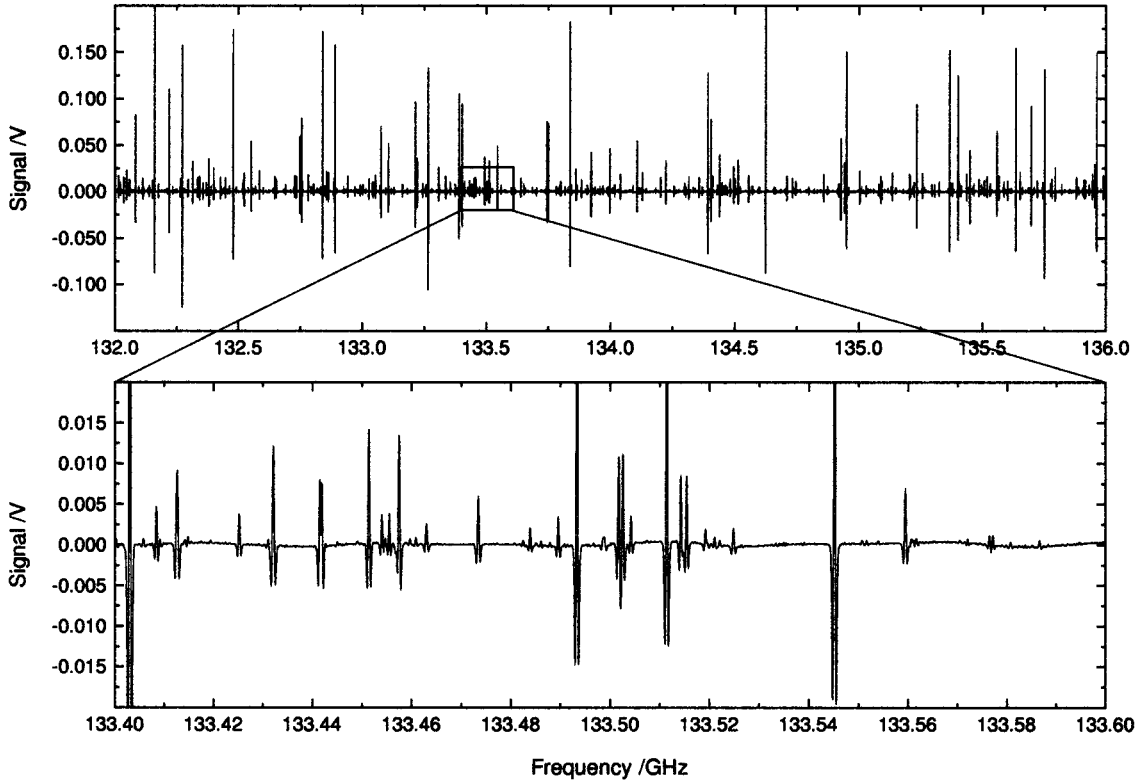


**Figure 1.** Segment of the spectrum of BrCNO, showing transitions for $J = 39 \leftarrow 38$, expanded in the lower trace by a factor of 10 in amplitude and a factor of 20 in frequency.

frequency to 10 kHz, whereas with the diode detectors, modulation frequencies of up to 100 kHz were realized. All spectra were recorded in 2*f* demodulation, providing approximately second derivatives of the absorption profile functions. The step width between two data points was chosen to be 25 kHz below 179 GHz and 50 kHz above 210 GHz; the integration time per data point was set to 100 ms in both cases. A scan of 20 000 data points covering 500 or 1000 MHz required about 63 min. Under similar experimental conditions, the millimeter-wave spectrum of ClCNO, synthesized by gaseous phase pyrolysis of dichloroformaldoxime $Cl_2CNOH$,[7] was recorded in the frequency ranges of 52−119, 159−179, and 210−230 GHz. These survey spectra were actually good enough for precision measurements of line positions with a statistical error of ±10 kHz.

All spectra of BrCNO and ClCNO were smoothed using the Savitzky-Golay algorithm[12] with smoothing windows of eleven points for the spectra recorded below 179 GHz and nine points for the spectra recorded above 210 GHz. Line positions in each case were determined utilizing an automated peak finding program.[13] Using separate measurements of rotational transitions of OCS, these line positions were finally corrected for a small (<20 kHz) frequency offset,[10] caused by an offset of the internal frequency standard of the synthesizer.

## Spectra and Assignment

A section of the smoothed survey spectrum of BrCNO is shown in Figure 1 in order to demonstrate the high density of lines and the large amount of data contained in each part of the recorded spectra. As illustrated in Figure 2, the density of lines is not quite as high in the survey spectrum of ClCNO, which is due in part to a 50% larger overall rotational constant and in part to the isotopic abundance ratio of 3:1 for $^{35}Cl$ and $^{37}Cl$, rather than 1:1 for $^{79}Br$ and $^{81}Br$.

The overall strategy for the assignment of the observed rotational transitions of $^{79}BrCNO$ and $^{81}BrCNO$ in the vibrational ground state and in thermally excited states of the low-lying BrCN bending mode was already discussed in our previous publication.[8] Because this strategy was of crucial importance for understanding the complex and apparently irregular spectra of both BrCNO and ClCNO, we nonetheless briefly repeat the discussion below.

In general, rotational transitions of XCNO were assigned in terms of a linear molecule with two degenerate bending modes, an XCN bending mode $\nu_5$, and a CNO bending mode $\nu_4$. Each bending mode is associated with a vibrational angular momentum with the quantum number $l_t$ ($t = 4$ or 5). The total vibrational angular momentum with the quantum number $k$ is the vector sum of the individual vibrational angular momenta. If only one bending mode $\nu_t$ is excited, we have $k = l_t$. In the rotating molecule, the degeneracy of the bending modes is lifted, and for each $k$, two components of different symmetry, $k^e$and $k^f$, may be distinguished, except in the case $k = l_t = 0$. It is important to keep in mind that all transitions of XCNO can also be assigned in terms of a nearly prolate asymmetric top molecule with an *in-plane* XCN bending mode $\nu_5^b$, an *in-plane* CNO bending mode $\nu_4^b$, and an *out-of-plane* CNO bending mode $\nu_6^b$. For bending levels in which exclusively the low-lying XCN bending mode is excited, the quantum numbers simply transform as follows:

$$K_a = l_5$$

$$v_5^b = \frac{v_5 - l_5}{2} \qquad (1)$$

All transitions discussed here in terms of rotational transitions of a linear molecule correspond to *a*-type rotational transitions of an asymmetric rotor, with $\Delta k = \Delta K_a = 0$.

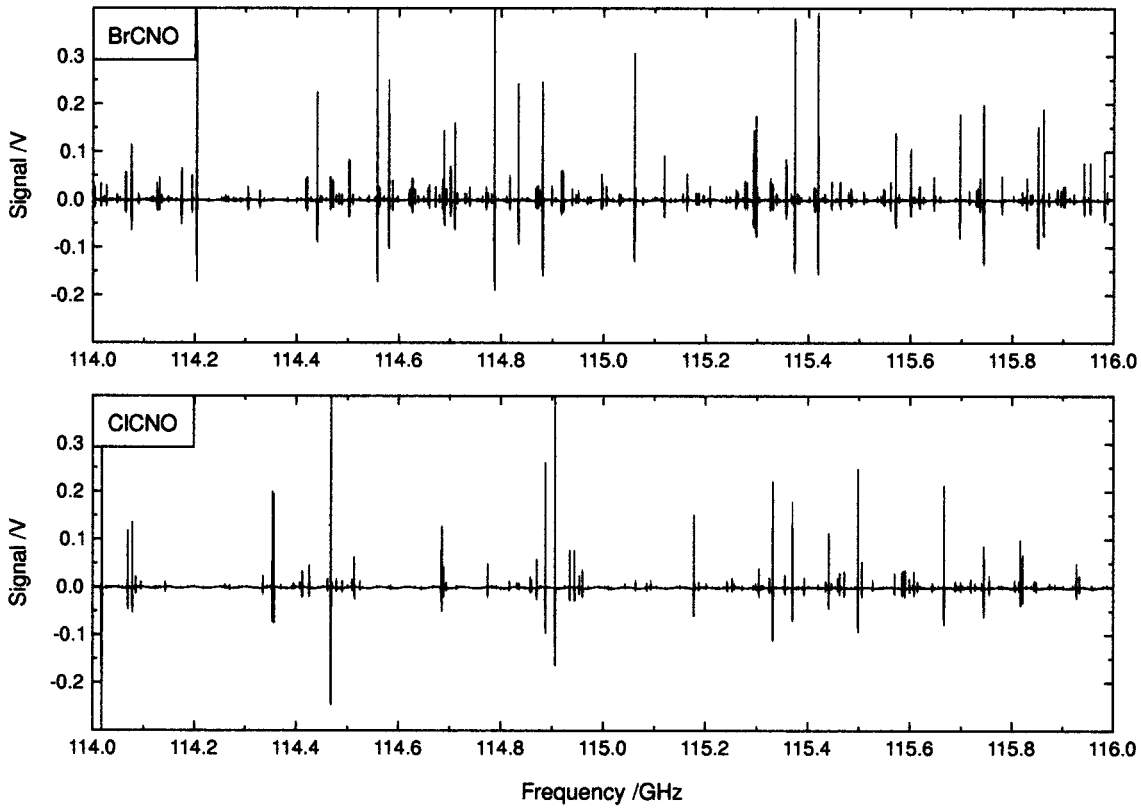


**Figure 2.** Segment of the rotational spectra of BrCNO and ClCNO, showing $J = 34 \leftarrow 33$ transitions for both isotopomers of BrCNO and $J = 23 \leftarrow 22$ transitions for both isotopomers of ClCNO.

The most intense rotational transitions were first classified into series in $J$, each series or pair of series corresponding to a single XCN bending level. Initially ignoring nuclear quadrupole splitting, the transition frequencies of each series were analyzed using a least-squares procedure by adjusting the coefficients in the conventional power series

$$\nu_0 = B_{ps}[2(J+1)] - D_{ps}[4(J+1)^3] + H_{ps}[6(J+1)^5 + 2(J+1)^3] + L_{ps}[8(J+1)^7 + 8(J+1)^5] \quad (2)$$

The final power series constants, as determined later after the nuclear quadrupole splitting had been analyzed, are summarized in Table 1. Several series were found to be perturbed by local resonances. As far as possible, the affected transitions were excluded from the fits, as were transitions with blended absorption profiles. The frequencies of the unsplit transitions are listed in the Supporting Information.

The $J$ values covered a range from 14 to 64 for BrCNO and from 10 to 43 for ClCNO. Line positions or $B_{ps}$ constants, intensities, and splittings of the lines all seemed at first to give contradictory indications instead of a self-consistent assignment. Finally, assignment of the value of $l_5 = k = K_a$ for each series was achieved by examining carefully the halogen nuclear quadrupole splitting. In contrast to $l$-type resonance splitting (or asymmetry splitting), which increases with $J$, nuclear quadrupole splitting decreases with $J$. In the case of BrCNO, bromine nuclear quadrupole splitting was at least partially resolved for the lowest observed transitions of each series. In the case of ClCNO, owing to a much smaller coupling constant, chlorine nuclear quadrupole splitting for $k \leq 1$ could only be resolved when the survey spectrum below 62 GHz was recorded at Doppler-limited resolution, i.e., with a lower sample pressure and with a reduced modulation deviation of 150 kHz. The characteristic dependence of the quadrupole splitting caused by the halogen nuclei in XCNO on $k = K_a$ is illustrated in Figure 3. Additionally, for $l_5 = 2$ and $l_5 = 3$, the assignment could be confirmed by examining the $l$-type resonance splitting. It is worth noting that this splitting was found to be considerably smaller than in the case of a regular linear molecule, and for $l_5 \geq 4$, it could not be resolved even in the 210−230 GHz range.

Once the value of $l_5$ was known for each series of rotational transitions, vibrational quantum numbers $v_5$ could unambiguously be assigned using relative intensities: For a given $l_5$, the most intense series or pair of series belongs to $v_5 = l_5$, the next most intense to $v_5 = l_5 + 2$, etc. For BrCNO, this procedure provided a very consistent but unusual assignment, which is shown in Figure 4 in the form of a Fortrat diagram for $^{81}$BrCNO.

Evidently, the sequence of series of rotational transitions in different BrCN bending levels of BrCNO as illustrated in Figure 4 is completely inconsistent with the sequence to be expected for a linear molecule. Furthermore, the sequence of transition series to be expected for a nearly prolate top molecule does not resemble the observed spectrum any more closely. The dependence of the rotational constants on $v_5$ and $l_5$ (or on $v_5^b$ and $K_a$) is, however, analogous to that found for the highly anharmonic CCC bending mode of carbon suboxide OCCCO,[14] though even more irregular. Except for considerably more bent molecules such as NCNCS[15] and HNCS,[16] BrCNO is the first molecule we have ever encountered where, in terms of a linear molecule, the rotational constant in the $v_5^{l_5} = 2^\circ$ level is considerably smaller than that of the vibrational ground state. The rotational constants in the $l_5 = 0$ levels of the fourth and higher excited BrCN bending states are increasingly larger than the rotational constant in the vibrational ground state, approaching the pattern for a linear molecule. Altogether, these results prove beyond doubt that BrCNO is an extremely quasilinear molecule with a

**TABLE 1: Halogen Nuclear Quadrupole Coupling Constants *eQq*, Asymmetry Constants *eQqη*, and Rotational Power Series Constants for the Unsplit Positions of the Rotational Transitions for $v_5 = n$ and $(v_4, v_5) = (1, n)$ Bending Levels of BrCNO and ClCNO[a]**

| $(v_4^{l_4}, v_5^{l_4})^k$ | *eQq*/MHz | *eQqη*/MHz | $B_{ps}$/MHz | $D_{ps}$/Hz | $H_{ps}/\mu$Hz | $L_{ps}$/nHz | $\sigma$/kHz |
|---|---|---|---|---|---|---|---|
| | | | $^{81}$BrCNO | | | | |
| $(0^0, 0^0)^{0e}$ | 551 (10) | | 1726.961767 (79) | 335.045 (39) | 736.2 (55) | | 9.4 |
| $(0^0, 1^1)^{1e}$ | 555.6[b] | −28[b] | 1730.936803 (78) | 264.342 (38) | 475.8 (54) | | 9.3 |
| $(0^0, 1^1)^{1f}$ | 555.6(26) | −49.8 (58) | 1736.378936 (73) | 302.226 (36) | 629.8 (50) | | 8.7 |
| $(0^0, 2^2)^{2e}$ | 551.7(76) | | 1741.19132 (22) | 265.09 (19) | 847 (65) | −36.0(71) | 14.6 |
| $(0^0, 2^2)^{2f}$ | 551.7(76) | | 1741.18716 (26) | 258.43 (22) | −200 (75) | 37.0(82) | 16.7 |
| $(0^0, 3^3)^{3e/f}$ | 548.6(47) | | 1748.632565 (95) | 254.808 (49) | 311.4 (71) | | 11.4 |
| $(0^0, 4^4)^{4e/f}$ | 546.9 (28) | | 1755.857123 (75) | 251.615 (37) | 279.8 (54) | | 8.4 |
| $(0^0, 5^5)^{5e/f}$ | 535.5 (19) | | 1762.861050 (64) | 251.149 (33) | 278.6 (48) | | 7.7 |
| $(0^0, 6^6)^{6e/f}$ | 530.3 (12) | | 1769.665937 (90) | 252.192 (46) | 262.7 (67) | | 10.8 |
| $(0^0, 7^7)^{7e/f}$ | 523.85 (91) | | 1776.297618 (72) | 254.523 (39) | 256.6 (60) | | 8.3 |
| $(0^0, 8^8)^{8e/f}$ | 518.61 (70) | | 1782.779269 (71) | 257.855 (37) | 248.3 (56) | | 8.3 |
| $(0^0, 9^9)^{9e/f}$ | 515.76 (95) | | 1789.131052 (75) | 262.246 (39) | 242.7 (59) | | 8.9 |
| $(0^0, 10^{10})^{10e/f}$ | 508.60 (44) | | 1795.36963 (11) | 267.613 (63) | 207.0 (97) | | 11.8 |
| $(0^0, 2^0)^{0e}$ | 556 (10) | | 1723.55074 (12) | 193.412 (63) | 1040.5 (87) | | 14.6 |
| $(0^0, 3^1)^{1e}$ | 553.3 (25) | −26.5 (55) | 1734.381356 (74) | 203.116 (37) | 453.4 (52) | | 8.8 |
| $(0^0, 3^1)^{1f}$ | 552.4 (32) | −47.6 (79) | 1740.397830 (85) | 228.687 (43) | 586.0 (62) | | 9.8 |
| $(0^0, 4^2)^{2e}$ | 546.7[b] | | 1747.397609 (79) | 247.010 (38) | 78.1 (53) | | 7.4 |
| $(0^0, 4^2)^{2f}$ | 546.7[b] | | 1747.39710 (13) | 223.245 (61) | 380.0 (81) | | 9.8 |
| $(0^0, 5^3)^{3e}$ | 542.1 (47) | | 1755.98941 (15) | 238.079 (87) | 159 (12) | | 15.1 |
| $(0^0, 5^3)^{3f}$ | 542.1 (47) | | 1755.98993 (12) | 238.722 (70) | 374.3 (97) | | 12.0 |
| $(0^0, 6^4)^{4e/f}$ | 525.9 (32) | | 1763.82687 (10) | 241.934 (52) | 236.1 (74) | | 11.3 |
| $(0^0, 7^5)^{5e/f}$ | 530.2 (15) | | 1771.183827 (64) | 246.010 (33) | 240.6 (48) | | 7.7 |
| $(0^0, 8^6)^{6e/f}$ | 525.3 (12) | | 1778.200662 (91) | 250.353 (50) | 248.3 (74) | | 10.2 |
| $(0^0, 9^7)^{7e/f}$ | 519.15 (91) | | 1784.961146 (68) | 254.886 (35) | 234.7 (53) | | 8.1 |
| $(0^0, 10^8)^{8e/f}$ | 512.2 (19) | | 1791.52040 (11) | 259.797 (63) | 211.1 (93) | | 13.3 |
| $(0^0, 4^0)^{0e}$ | 546.5 (88) | | 1738.275812 (82) | 118.991 (41) | 122.7 (57) | | 9.9 |
| $(0^0, 5^1)^{1e}$ | 547.7 (33) | −29.9 (75) | 1744.582257 (60) | 166.388 (30) | 284.9 (44) | | 7.2 |
| $(0^0, 5^1)^{1f}$ | 547.7[b] | −49[b] | 1751.92655 (12) | 186.289 (61) | 240.9 (87) | | 13.9 |
| $(0^0, 6^2)^{2e}$ | 552 (12) | | 1757.292220 (99) | 277.390 (50) | −67.0 (71) | | 11.0 |
| $(0^0, 6^2)^{2f}$ | 552 (12) | | 1757.291402 (99) | 195.542 (50) | 312.6 (71) | | 11.1 |
| $(0^0, 7^3)^{3e}$ | 535.5 (47) | | 1765.530810 (99) | 237.114 (49) | −134.7 (68) | | 10.4 |
| $(0^0, 7^3)^{3f}$ | 535.5 (47) | | 1765.53028 (11) | 237.067 (56) | 421.7 (75) | | 12.4 |
| $(0^0, 8^4)^{4e/f}$ | 531.8 (34) | | 1773.20138 (10) | 242.439 (51) | 166.8 (74) | | 10.0 |
| $(0^0, 9^5)^{5e/f}$ | 524.2 (18) | | 1780.43794 (42) | 247.25 (80) | −2070 (470) | | 7.7[c] |
| $(0^0, 10^6)^{6e/f}$ | 520.2 (12) | | 1786.97935 (27) | 290.29 (30) | −3860 (100) | | 12.7[c] |
| $(0^0, 6^0)^{0e}$ | 534.4 (88) | | 1753.18727 (14) | 92.100 (70) | 366 (10) | | 16.1 |
| $(0^0, 8^2)^{2e}$ | 534.3 (76) | | 1768.38594 (11) | 372.453 (60) | −1053.7 (94) | | 12.4[c] |
| $(0^0, 8^2)^{2f}$ | 528.7 (76) | | 1768.38471 (23) | 183.57 (24) | −709 (79) | | 11.7[b] |
| $(0^0, 9^3)^{3e}$ | 531.7 (47) | | 1775.97802 (22) | 254.86 (21) | −786 (80) | −40.3 (93) | 13.4 |
| $(0^0, 9^3)^{3f}$ | 531.7 (47) | | 1775.97675 (11) | 254.056 (55) | 952.7 (81) | | 10.0 |
| $(0^0, 10^4)^{4e/f}$ | 513.8 (55) | | 1783.17430 (39) | 255.79 (26) | −402 (52) | | 14.5[c] |
| | | | $^{79}$BrCNO | | | | |
| $(0^0, 0^0)^{0e}$ | 656.8 (88) | | 1739.930056 (77) | 339.870 (38) | 757.4 (54) | | 9.4 |
| $(0^0, 1^1)^{1e}$ | 653.9 (28) | −39.1 (60) | 1743.917684 (72) | 267.950 (35) | 485.9 (49) | | 8.8 |
| $(0^0, 1^1)^{1f}$ | 654.3 (26) | −46.4 (55) | 1749.437299 (84) | 306.612 (43) | 640.9 (62) | | 10.2 |
| $(0^0, 2^2)^{2e}$ | 655.0 (76) | | 1754.26779 (27) | 269.12 (24) | 952 (83) | −46.4 (93) | 17.7 |
| $(0^0, 2^2)^{2f}$ | 655.0 (76) | | 1754.26353 (27) | 262.26 (23) | −155 (81) | 34.3 (91) | 17.3 |
| $(0^0, 3^3)^{3e/f}$ | 654.6 (47) | | 1761.76427 (11) | 258.536 (59) | 334.8 (85) | | 13.8 |
| $(0^0, 4^4)^{4e/f}$ | 644.9 (28) | | 1769.042618 (75) | 255.321 (37) | 299.0 (53) | | 8.2 |
| $(0^0, 5^5)^{5e/f}$ | 640.8 (19) | | 1776.098245 (77) | 254.760 (41) | 287.3 (62) | | 9.0 |
| $(0^0, 6^6)^{6e/f}$ | 634.4 (12) | | 1782.953487 (62) | 255.782 (33) | 264.0 (50) | | 7.2 |
| $(0^0, 7^7)^{7e/f}$ | 627.74 (91) | | 1789.634376 (65) | 258.176 (35) | 262.0 (53) | | 7.6 |
| $(0^0, 8^8)^{8e/f}$ | 621.08 (70) | | 1796.164107 (81) | 261.560 (43) | 249.5 (64) | | 9.5 |
| $(0^0, 9^9)^{9e/f}$ | 614.73 (55) | | 1802.562859 (96) | 265.941 (52) | 237.6 (81) | | 10.9 |
| $(0^0, 10^{10})^{10e/f}$ | 608.67 (44) | | 1808.847980 (98) | 271.526 (54) | 219.0 (84) | | 10.5 |
| $(0^0, 2^0)^{0e}$ | 665.6 (88) | | 1736.490309 (94) | 195.945 (47) | 1056.7 (65) | | 11.4 |
| $(0^0, 3^1)^{1e}$ | 649.5[b] | −43[b] | 1747.38171 (11) | 205.701 (52) | 448.2 (68) | | 8.1 |
| $(0^0, 3^1)^{1f}$ | 649.5 (48) | −43 (10) | 1753.48403 (10) | 231.939 (53) | 603.0 (77) | | 12.8 |
| $(0^0, 4^2)^{2e}$ | 660.5 (88) | | 1760.51660 (15) | 250.684 (77) | 69 (10) | | 15.3 |
| $(0^0, 4^2)^{2f}$ | 658.5 (88) | | 1760.51666 (13) | 226.515 (66) | 410.6 (92) | | 13.2 |
| $(0^0, 5^3)^{3e}$ | 648.3 (56) | | 1769.17393 (15) | 241.633 (89) | 179 (12) | | 14.4 |
| $(0^0, 5^3)^{3f}$ | 648.3 (56) | | 1769.17438 (13) | 242.231 (80) | 392 (11) | | 12.9 |
| $(0^0, 6^4)^{4e/f}$ | 643.5 (28) | | 1777.070972 (84) | 245.488 (43) | 246.4 (63) | | 8.9 |
| $(0^0, 7^5)^{5e/f}$ | 634.6 (18) | | 1784.48343 (10) | 249.527 (56) | 243.6 (84) | | 12.7 |
| $(0^0, 8^6)^{6e/f}$ | 628.1 (12) | | 1791.55344 (10) | 253.841 (58) | 233.4 (85) | | 12.1 |
| $(0^0, 9^7)^{7e/f}$ | 621.24 (91) | | 1798.365419 (64) | 258.619 (35) | 243.9 (51) | | 7.1 |
| $(0^0, 10^8)^{8e/f}$ | 614.52 (70) | | 1804.974455 (65) | 263.661 (35) | 227.6 (53) | | 7.1 |
| $(0^0, 4^0)^{0e}$ | 650.1 (88) | | 1751.33195 (10) | 120.370 (54) | 133.2 (78) | | 12.9 |
| $(0^0, 5^1)^{1e}$ | 638.0 (41) | −56.4 (87) | 1757.657812 (97) | 168.516 (49) | 296.9 (71) | | 11.4 |

**TABLE 1: Continued**

| $(v_4^{l_4}, v_5^{l_4})^k$ | $eQq$/MHz | $eQq\eta$/MHz | $B_{ps}$/MHz | $D_{ps}$/Hz | $H_{ps}/\mu$Hz | $L_{ps}$/nHz | $\sigma$/kHz |
|---|---|---|---|---|---|---|---|
| $(0^0, 5^1)^{1f}$ | 638.5 (34) | −52.3 (71) | 1765.107396 (96) | 188.814 (50) | 247.6 (72) | | 11.1 |
| $(0^0, 6^2)^{2e}$ | 620 (12) | | 1770.487980 (82) | 282.120 (42) | −75.2 (59) | | 9.1 |
| $(0^0, 6^2)^{2f}$ | 657 (12) | | 1770.48722 (11) | 198.091 (60) | 315.7 (86) | | 13.3 |
| $(0^0, 7^3)^{3e}$ | 640.7 (47) | | 1778.78936 (13) | 240.702 (64) | −137.0 (91) | | 13.2 |
| $(0^0, 7^3)^{3f}$ | 640.7 (47) | | 1778.78880 (13) | 240.625 (60) | 436.1 (82) | | 12.8 |
| $(0^0, 8^4)^{4e/f}$ | 635.8 (28) | | 1786.51860 (14) | 246.064 (73) | 175 (10) | | 14.4 |
| $(0^0, 9^5)^{5e/f}$ | 627.1 (18) | | 1793.80957 (26) | 251.39 (40) | −1250 (180) | | 8.4[c] |
| $(0^0, 10^6)^{6e/f}$ | 621.5 (12) | | 1800.34159 (20) | 301.39 (23) | −5419 (77) | | 9.9[c] |
| $(0^0, 6^0)^{0e}$ | 636.6 (88) | | 1766.35618 (10) | 92.403 (56) | 382.2 (82) | | 12.9 |
| $(0^0, 8^2)^{2e}$ | 638.8 (88) | | 1781.68243 (16) | 378.35 (12) | −879 (27) | | 12.3[c] |
| $(0^0, 8^2)^{2f}$ | 630.2 (88) | | 1781.68103 (28) | 184.61 (30) | −418 (97) | | 13.8[c] |
| $(0^0, 9^3)^{3e}$ | 637.3 (88) | | 1789.32063 (17) | 258.97 (16) | −783 (59) | −48.0 (68) | 10.8 |
| $(0^0, 9^3)^{3f}$ | 637.3 (88) | | 1789.31943 (10) | 258.057 (49) | 963.5 (68) | | 9.3 |
| $(0^0, 10^4)^{4e/f}$ | 628.7 (40) | | 1796.56277 (55) | 257.34 (32) | −773 (62) | | 13.6[c] |
| | | | $^{37}$ClCNO | | | | |
| $(0^0, 0^0)^{0e}$ | −63.16[b] | | 2511.44612 (16) | 583.12 (21) | 1555 (62) | | 10.5 |
| $(0^0, 1^1)^{1e}$ | −62.52[b] | | 2514.96929 (16) | 452.60 (20) | 903 (59) | | 10.0 |
| $(0^0, 1^1)^{1f}$ | −62.52[b] | | 2524.99915 (13) | 533.52 (16) | 1287 (49) | | 8.3 |
| $(0^0, 2^2)^{2e}$ | −61.89[b] | | 2529.97768 (22) | 458.85 (24) | 856 (65) | | 9.1 |
| $(0^0, 2^2)^{2f}$ | −61.89[b] | | 2529.97862 (12) | 444.607 (36) | | | 9.1 |
| $(0^0, 3^3)^{3e/f}$ | −62.2 (19) | | 2539.96170 (18) | 442.54 (23) | 576 (66) | | 11.3 |
| $(0^0, 4^4)^{4e/f}$ | −61.1 (11) | | 2549.69044 (13) | 437.84 (16) | 520 (48) | | 8.2 |
| $(0^0, 5^5)^{5e/f}$ | −59.20 (70) | | 2559.13665 (18) | 437.01 (25) | 451 (75) | | 10.1 |
| $(0^0, 6^6)^{6e/f}$ | −59.66 (48) | | 2568.32111 (17) | 439.46 (23) | 550 (69) | | 10.5 |
| $(0^0, 7^7)^{7e/f}$ | −58.62 (35) | | 2577.27357 (10) | 443.66 (13) | 549 (41) | | 6.0 |
| $(0^0, 8^8)^{8e/f}$ | −58.05 (27) | | 2586.02329 (10) | 449.39 (14) | 487 (44) | | 6.2 |
| $(0^0, 9^9)^{9e/f}$ | −57.44 (21) | | 2594.59707 (11) | 456.93 (17) | 468 (54) | | 5.7 |
| $(0^0, 10^{10})^{10e/f}$ | −56.79[b] | | 2603.01647 (33) | 465.18 (40) | 150 (120) | | 15.9 |
| $(0^0, 2^0)^{0e}$ | −62.51[b] | | 2504.22593 (13) | 354.09 (16) | 2390 (48) | | 8.2 |
| $(0^0, 3^1)^{1e}$ | −61.86[b] | | 2518.12389 (18) | 351.88 (23) | 928 (66) | | 11.3 |
| $(0^0, 3^1)^{1f}$ | −61.86[b] | | 2529.02682 (13) | 407.15 (17) | 1318 (50) | | 8.6 |
| $(0^0, 4^2)^{2e}$ | −61.22[b] | | 2537.43746 (20) | 445.84 (25) | −166 (72) | | 11.9 |
| $(0^0, 4^2)^{2f}$ | −61.22[b] | | 2537.43760 (16) | 389.32 (20) | 937 (59) | | 9.7 |
| $(0^0, 5^3)^{3e/f}$ | −61.2 (19) | | 2549.25720 (16) | 420.28 (20) | 468 (59) | | 10.1 |
| $(0^0, 6^4)^{4e/f}$ | −60.5 (11) | | 2559.98229 (22) | 425.41 (31) | 364 (94) | | 12.6 |
| $(0^0, 7^5)^{5e/f}$ | −58.62 (70) | | 2570.00326 (16) | 432.45 (21) | 501 (65) | | 9.9 |
| $(0^0, 8^6)^{6e/f}$ | −58.66[b] | | 2579.51846 (18) | 439.37 (23) | 441 (68) | | 9.8 |
| $(0^0, 9^7)^{7e/f}$ | −58.01[b] | | 2588.64683 (39) | 446.97 (50) | 270 (150) | | 21.7 |
| $(0^0, 10^8)^{8e/f}$ | −57.37[b] | | 2597.46507 (16) | 456.28 (20) | 266 (59) | | 7.2 |
| $(0^0, 4^0)^{0e}$ | −62.28[b] | | 2523.75564 (14) | 189.74 (18) | 561 (53) | | 9.1 |
| $(0^0, 5^1)^{1e}$ | −61.54[b] | | 2531.27203 (14) | 279.54 (17) | 681 (51) | | 8.6 |
| $(0^0, 5^1)^{1f}$ | −61.54[b] | | 2544.50902 (14) | 321.10 (18) | 542 (52) | | 8.7 |
| $(0^0, 6^2)^{2e}$ | −60.80[b] | | 2550.43584 (18) | 535.42 (23) | −564 (68) | | 11.4 |
| $(0^0, 6^2)^{2f}$ | −60.80[b] | | 2550.43521 (15) | 334.41 (19) | 607 (57) | | 9.6 |
| $(0^0, 7^3)^{3e}$ | −60.8 (19) | | 2561.37735 (36) | 358.44 (79) | −9910 (600) | 840 (140) | 10.2 |
| $(0^0, 7^3)^{3f}$ | −60.8 (19) | | 2561.37858 (18) | 363.11 (25) | −4489 (74) | | 9.5 |
| $(0^0, 8^4)^{4e/f}$ | −59.1 (11) | | 2572.36840 (16) | 433.11 (21) | 376 (65) | | 8.9 |
| $(0^0, 9^5)^{5e/f}$ | −58.59[b] | | 2582.24077 (20) | 442.46 (22) | 99 (62) | | 8.6 |
| $(0^0, 10^6)^{6e/f}$ | −57.86[b] | | 2591.7090 (88) | 457.3 (43) | | | 49.9 |
| $(0^0, 6^0)^{0e}$ | −60.95[b] | | 2544.41843 (34) | 115.83 (65) | 4960 (430) | −560 (92) | 10.8 |
| $(0^0, 7^1)^{1e}$ | −60.02[b] | | 2546.74945 (17) | 239.20 (21) | 1177 (63) | | 10.8 |
| $(0^0, 7^1)^{1f}$ | −60.02[b] | | 2562.70607 (13) | 286.41 (18) | −921 (57) | | 8.1 |
| $(0^0, 8^2)^{2e}$ | −59.10[b] | | 2564.93562 (36) | 658.64 (74) | −16260 (510) | 2130 (120) | 11.4 |
| $(0^0, 8^2)^{2f}$ | −59.10[b] | | 2564.93320 (26) | 208.35 (53) | −8730 (370) | 735 (83) | 7.7 |
| $(1^1, 1^1)^{0f}$ | −62.52[b] | | 2522.53076 (15) | 573.33 (18) | 2675 (54) | | 9.1 |
| $(1^1, 0^0)^{1e}$ | −63.16[b] | | 2510.60996 (15) | 527.92 (20) | 595 (58) | | 9.9 |
| $(1^1, 0^0)^{1f}$ | −63.16[b] | | 2513.04070 (28) | 622.97 (36) | 510 (100) | | 17.7 |
| $(1^1, 1^1)^{2e}$ | −62.52[b] | | 2520.72220 (16) | 549.53 (21) | 1372 (63) | | 9.4 |
| $(1^1, 1^1)^{2f}$ | −62.52[b] | | 2520.72180 (10) | 419.408 (26) | | | 9.0 |
| $(1^1, 2^2)^{3e/f}$ | −61.89[b] | | 2531.30427 (38) | 517.55 (47) | 5640 (130) | | 21.4 |
| $(1^1, 3^3)^{4e/f}$ | −62.4 (11) | | 2540.97757 (18) | 442.03 (22) | 615 (65) | | 11.1 |
| $(1^1, 1^1)^{0e}$ | | | 2516.86256 (17) | 415.65 (21) | 1278 (62) | | 10.7 |
| $(1^1, 2^2)^{1e}$ | | | 2526.82075 (16) | 363.70 (21) | 242 (61) | | 10.0 |
| $(1^1, 2^2)^{1f}$ | | | 2528.41784 (17) | 481.71 (22) | 1034 (65) | | 11.1 |
| $(1^1, 3^3)^{2e}$ | | | 2538.73208 (30) | 430.98 (30) | −617 (82) | | 11.1 |
| $(1^1, 3^3)^{2f}$ | | | 2538.73296 (42) | 420.20 (43) | −640 (120) | | 15.6 |
| $(1^1, 2^1)^{1e}$ | | | 2505.85078 (18) | 355.99 (24) | 3580 (70) | | 10.9 |
| $(1^1, 2^1)^{1f}$ | | | 2507.36350 (19) | 293.39 (24) | 3394 (71) | | 12.1 |
| $(1^1, 3^1)^{2e}$ | | | 2518.79772 (56) | 427.5 (12) | 64 (610) | | 13.8[c] |
| $(1^1, 3^1)^{2f}$ | | | 2518.79795 (56) | 429.3 (12) | 3040 (610) | | 13.8[c] |

**TABLE 1: Continued**

| $(v_4^{l_4}, v_5^{l_5})^k$ | $eQq$/MHz | $eQq\eta$/MHz | $B_{ps}$/MHz | $D_{ps}$/Hz | $H_{ps}$/$\mu$Hz | $L_{ps}$/nHz | $\sigma$/kHz |
|---|---|---|---|---|---|---|---|
| | | | $^{35}$ClCNO | | | | |
| $(0^0, 0^0)^{0e}$ | −80.94[b] | | 2572.78179 (17) | 609.85 (22) | 1801 (67) | | 10.0 |
| $(0^0, 1^1)^{1e}$ | −80.02[b] | | 2576.29749 (12) | 471.97 (15) | 1017 (47) | | 7.0 |
| $(0^0, 1^1)^{1f}$ | −80.02[b] | | 2586.77624 (13) | 557.98 (18) | 1390 (54) | | 8.1 |
| $(0^0, 2^2)^{2e}$ | −79.10[b] | | 2591.76974 (27) | 479.16 (30) | 902 (86) | | 11.0 |
| $(0^0, 2^2)^{2f}$ | −79.10[b] | | 2591.77064 (10) | 463.838 (30) | | | 7.9 |
| $(0^0, 3^3)^{3e/f}$ | −78.5 (15) | | 2601.98847 (15) | 462.14 (21) | 594 (65) | | 9.9 |
| $(0^0, 4^4)^{4e/f}$ | −76.68 (82) | | 2611.94396 (11) | 457.55 (15) | 594 (47) | | 7.2 |
| $(0^0, 5^5)^{5e/f}$ | −76.69 (52) | | 2621.60930 (20) | 457.07 (28) | 612 (89) | | 11.7 |
| $(0^0, 6^6)^{6e/f}$ | −75.44 (36) | | 2631.00585 (12) | 459.06 (17) | 507 (55) | | 7.5 |
| $(0^0, 7^7)^{7e/f}$ | −74.47 (26) | | 2640.16484 (13) | 463.60 (19) | 527 (62) | | 7.8 |
| $(0^0, 8^8)^{8e/f}$ | −73.53 (20) | | 2649.11643 (13) | 469.73 (18) | 473 (58) | | 7.3 |
| $(0^0, 9^9)^{9e/f}$ | −72.59 (16) | | 2657.88792 (14) | 478.17 (19) | 604 (62) | | 8.4 |
| $(0^0, 10^{10})^{10e/f}$ | −71.76 (17) | | 2666.50203 (14) | 487.26 (19) | 347 (62) | | 7.5 |
| $(0^0, 11^{11})^{11e/f}$ | −70.79 (19) | | 2674.97991 (23) | 499.45 (31) | 379 (99) | | 12.9 |
| $(0^0, 12^{12})^{12e/f}$ | −69.87[b] | | 2683.33849 (27) | 514.63 (32) | 4390 (100) | | 7.9[c] |
| $(0^0, 2^0)^{0e}$ | −80.11[b] | | 2565.41223 (15) | 368.57 (20) | 2544 (61) | | 9.1 |
| $(0^0, 3^1)^{1e}$ | −79.18[b] | | 2579.51626 (13) | 366.50 (17) | 1033 (51) | | 7.7 |
| $(0^0, 3^1)^{1f}$ | −79.18[b] | | 2590.90929 (12) | 425.11 (15) | 1405 (48) | | 7.1 |
| $(0^0, 4^2)^{2e}$ | −78.25[b] | | 2599.40004 (18) | 467.57 (23) | −264 (70) | | 9.9 |
| $(0^0, 4^2)^{2f}$ | −78.25[b] | | 2599.39991 (17) | 405.62 (22) | 871 (67) | | 9.5 |
| $(0^0, 5^3)^{3e/f}$ | −77.7 (15) | | 2611.49709 (20) | 439.55 (27) | 480 (84) | | 12.9 |
| $(0^0, 6^4)^{4e/f}$ | −75.91 (82) | | 2622.47309 (16) | 445.72 (23) | 620 (73) | | 9.7 |
| $(0^0, 7^5)^{5e/f}$ | −75.80 (52) | | 2632.72553 (19) | 451.85 (26) | 384 (84) | | 11.4 |
| $(0^0, 8^6)^{6e/f}$ | −74.53 (36) | | 2642.45980 (12) | 459.63 (17) | 469 (56) | | 7.0 |
| $(0^0, 9^7)^{7e/f}$ | −73.57 (26) | | 2651.79591 (14) | 468.52 (19) | 508 (62) | | 8.3 |
| $(0^0, 10^8)^{8e/f}$ | −72.66 (20) | | 2660.81081 (15) | 477.85 (21) | 371 (68) | | 9.1 |
| $(0^0, 11^9)^{9e/f}$ | −71.78 (16) | | 2669.54903 (22) | 490.91 (31) | 333 (98) | | 12.2 |
| $(0^0, 12^{10})^{10e/f}$ | −70.83[b] | | 2677.776 (19) | 969 (61) | $313 \times 10^3$ | $-337 \times 10^3$ | 77.0[c] |
| $(0^0, 4^0)^{0e}$ | −79.81[b] | | 2585.44185 (12) | 195.85 (16) | 678 (49) | | 7.2 |
| $(0^0, 5^1)^{1e}$ | −78.76[b] | | 2592.96306 (12) | 290.93 (16) | 956 (50) | | 6.8 |
| $(0^0, 5^1)^{1f}$ | −78.76[b] | | 2606.80031 (14) | 334.33 (18) | 535 (55) | | 8.2 |
| $(0^0, 6^2)^{2e}$ | −77.71[b] | | 2612.70019 (18) | 566.89 (23) | −687 (70) | | 10.1 |
| $(0^0, 6^2)^{2f}$ | −77.71[b] | | 2612.69969 (16) | 348.67 (21) | 662 (64) | | 8.9 |
| $(0^0, 7^3)^{3e}$ | −76.9 (15) | | 2624.06179 (24) | 409.87 (55) | −5230 (420) | 440 (100) | 8.0 |
| $(0^0, 7^3)^{3f}$ | −76.9 (15) | | 2624.06213 (16) | 412.37 (24) | −1314 (76) | | 9.1 |
| $(0^0, 8^4)^{4e/f}$ | −75.15 (82) | | 2635.14603 (21) | 453.15 (30) | 149 (96) | | 12.2 |
| $(0^0, 9^5)^{5e/f}$ | −74.76 (52) | | 2645.23743 (19) | 464.46 (27) | −545 (88) | | 11.0 |
| $(0^0, 10^6)^{6e/f}$ | −73.56 (36) | | 2654.90752 (17) | 476.52 (24) | 700 (76) | | 10.2 |
| $(0^0, 11^7)^{7e/f}$ | −72.45 (26) | | 2664.08899 (17) | 483.77 (23) | 195 (73) | | 9.9 |
| $(0^0, 12^8)^{8e/f}$ | −71.43[b] | | 2672.9313 (10) | 492.1 (18) | −12640 (950) | | 16.2[c] |
| $(0^0, 6^0)^{0e}$ | −78.11[b] | | 2606.54845 (21) | 104.65 (46) | 2460 (330) | −215 (74) | 7.5 |
| $(0^0, 7^1)^{1e}$ | −76.82[b] | | 2608.74635 (15) | 247.94 (20) | 1203 (60) | | 8.9 |
| $(0^0, 7^1)^{1f}$ | −76.82[b] | | 2625.41911 (15) | 299.95 (21) | −1241 (65) | | 8.4 |
| $(0^0, 8^2)^{2e}$ | −75.54[b] | | 2627.68928 (34) | 734.76 (72) | −11490 (510) | 1690 (120) | 9.3 |
| $(0^0, 8^2)^{2f}$ | −75.54[b] | | 2627.68693 (31) | 241.84 (66) | −5670 (470) | 600 (110) | 8.5 |
| $(0^0, 9^3)^{3e}$ | −74.3 (15) | | 2638.70302 (20) | 492.36 (28) | −3601 (93) | | 11.5 |
| $(0^0, 9^3)^{3f}$ | −74.3 (15) | | 2638.70178 (21) | 492.08 (30) | 3376 (98) | | 12.2 |
| $(0^0, 10^4)^{4e/f}$ | −72.99 (82) | | 2648.37317 (26) | 524.72 (40) | −5200 (130) | | 14.3 |
| $(1^1, 1^1)^{0f}$ | −80.02[b] | | 2584.15650 (14) | 601.64 (19) | 2998 (57) | | 8.5 |
| $(1^1, 0^0)^{1e}$ | −80.94[b] | | 2571.90003 (17) | 550.48 (22) | 735 (68) | | 9.1 |
| $(1^1, 0^0)^{1f}$ | −80.94[b] | | 2574.46592 (16) | 659.51 (21) | 2003 (65) | | 9.7 |
| $(1^1, 1^1)^{2e}$ | −80.02[b] | | 2582.30367 (20) | 574.49 (25) | 1471 (76) | | 11.1 |
| $(1^1, 1^1)^{2f}$ | −80.02[b] | | 2582.30318 (10) | 434.755 (36) | | | 11.2 |
| $(1^1, 2^2)^{3e/f}$ | −79.5 (25) | | 2592.97310 (19) | 510.19 (25) | 3261 (76) | | 11.3 |
| $(1^1, 3^3)^{4e/f}$ | −77.66 (82) | | 2603.03229 (14) | 461.77 (19) | 708 (59) | | 9.0 |
| $(1^1, 4^4)^{5e/f}$ | −77.47 (52) | | 2613.15647 (20) | 455.63 (27) | 526 (84) | | 12.6 |
| $(1^1, 5^5)^{6e/f}$ | −76.40 (36) | | 2623.00665 (13) | 453.95 (18) | 576 (57) | | 7.4 |
| $(1^1, 1^1)^{0e}$ | −80.02[b] | | 2578.30775 (16) | 431.57 (21) | 1356 (64) | | 9.5 |
| $(1^1, 2^2)^{1e}$ | −79.10[b] | | 2588.47526 (15) | 377.99 (19) | 73 (59) | | 8.7 |
| $(1^1, 2^2)^{1f}$ | −79.10[b] | | 2590.11599 (15) | 504.73 (20) | 1032 (61) | | 9.0 |
| $(1^1, 3^3)^{2e}$ | −78.17[b] | | 2600.69790 (32) | 450.55 (32) | −732 (90) | | 10.7 |
| $(1^1, 3^3)^{2f}$ | −78.17[b] | | 2600.69855 (47) | 438.29 (47) | −830 (130) | | 15.6 |
| $(1^1, 4^4)^{3e/f}$ | −77.5 (15) | | 2611.11728 (12) | 446.42 (17) | 738 (55) | | 7.4 |
| $(1^1, 5^5)^{4e/f}$ | −75.91 (81) | | 2620.97995 (16) | 445.72 (23) | 1239 (73) | | 9.6 |
| $(1^1, 2^0)^{1e}$ | −80.11[b] | | 2567.12303 (16) | 369.78 (21) | 4079 (63) | | 9.4 |
| $(1^1, 2^0)^{1f}$ | −80.11[b] | | 2568.74586 (19) | 300.35 (25) | 3958 (76) | | 11.3 |
| $(1^1, 3^1)^{2e}$ | −79.18[b] | | 2580.43329 (28) | 454.65 (36) | 1580 (110) | | 15.8 |
| $(1^1, 3^1)^{2f}$ | −79.18[b] | | 2580.42889 (35) | 446.22 (45) | −50 (40) | | 18.9 |
| $(1^1, 4^2)^{3e/f}$ | −80.1 (19) | | 2591.05751 (16) | 437.37 (21) | 896 (66) | | 9.0 |
| $(1^1, 5^3)^{4e/f}$ | −77.52 (82) | | 2601.77640 (30) | 396.88 (62) | 8170 (310) | | 11.0[c] |

[a] The standard deviation $\sigma$ of the power series fit is given in the last column. [b] Estimated. See text. [c] Perturbed. See text.

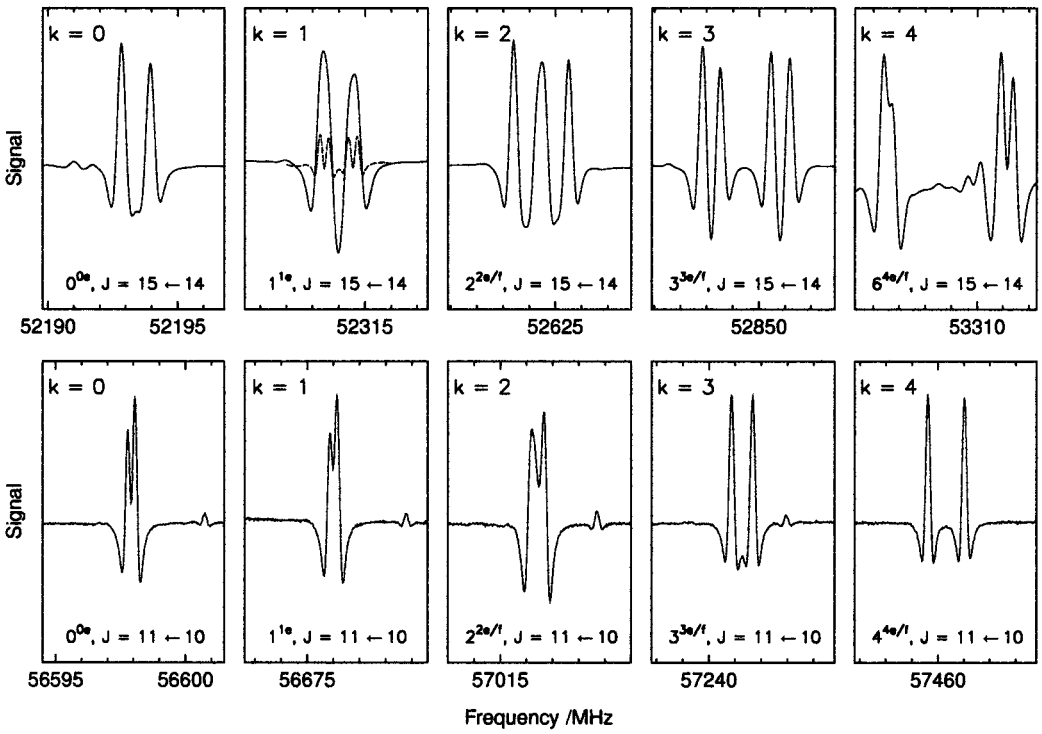


**Figure 3.** Nuclear quadrupole splitting of rotational transitions of $^{81}$BrCNO (upper row) and $^{35}$ClCNO (lower row). Transitions of $^{81}$BrCNO were recorded with a modulation deviation of 250 kHz; transitions of $^{35}$ClCNO were recorded with a reduced modulation deviation of 150 kHz. The dashed curve represents a $k = 1$ transition of $^{81}$BrCNO recorded under similar conditions as the transitions of $^{35}$ClCNO.

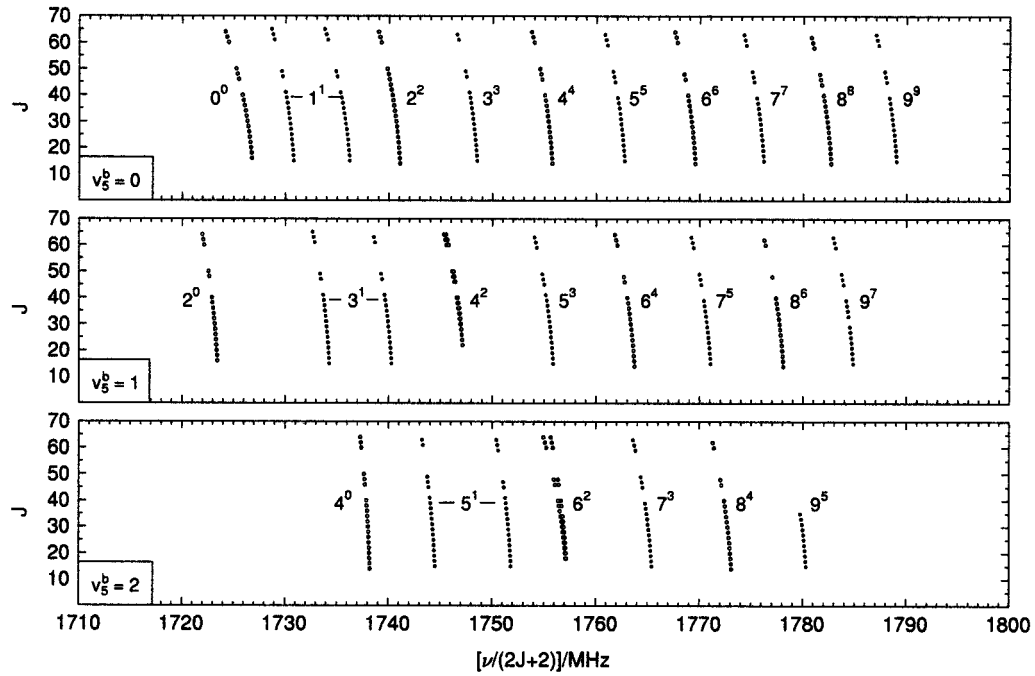


**Figure 4.** Fortrat diagram of rotational transitions of $^{81}$BrCNO in excited states of the BrCN bending mode. The series are labeled in terms of a linear molecule, i.e., $v_5^{l_5} \equiv v_5^k$. In terms of a nearly prolate top molecule, the first row of series belongs to the ground state ($v_5^b = 0$), the second row to the first excited state ($v_5{}^b = 1$), and the third row to the second excited state ($v_5^b = 2$) of a one-dimensional BrCN bending mode, whereas $K_a$ is identical to $l_5$. Note that in all Fortrat diagrams only every other transition of each series is shown.

highly anharmonic BrCN bending potential. The very anomalous position of the $v_5^{l_5} = 2°$ transitions indicates that the height of the barrier to linearity reaches roughly the term value of the $v_5^{l_5} = 2°$ excited bending level. Note that in terms of a nearly prolate top this level is the $K_a = 0$ rotational level of molecules in the first excited bending state.

As illustrated in Figure 5, the assignment obtained for both isotopomers of ClCNO is very similar to that obtained for the two isotopomers of BrCNO, which makes ClCNO another extremely quasilinear molecule. Again, the height of the barrier to linearity reaches approximately the term value of the $l_5 = 0$ level of the second excited bending state. The overall deviations from the limiting case of a linear molecule, however, are even more pronounced than in the case of BrCNO.

For both BrCNO and ClCNO, a large number of additional series of rotational transitions were observed, which belong

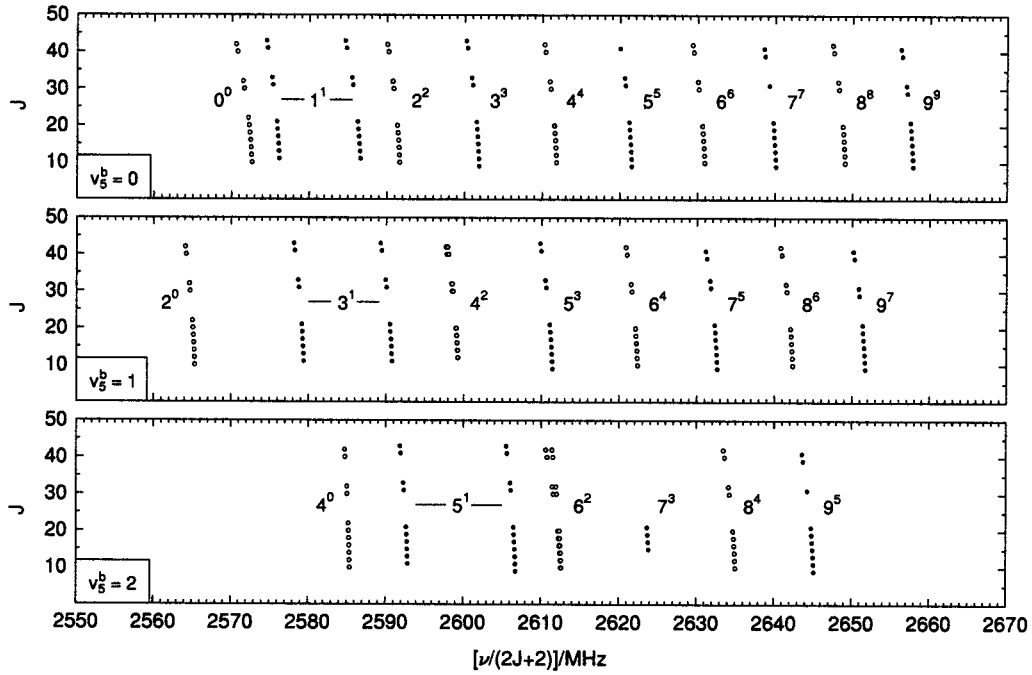


**Figure 5.** Fortrat diagram of rotational transitions of $^{35}$ClCNO in excited states of the ClCN bending mode. All series are labeled and arranged like those of $^{81}$BrCNO in Figure 4.

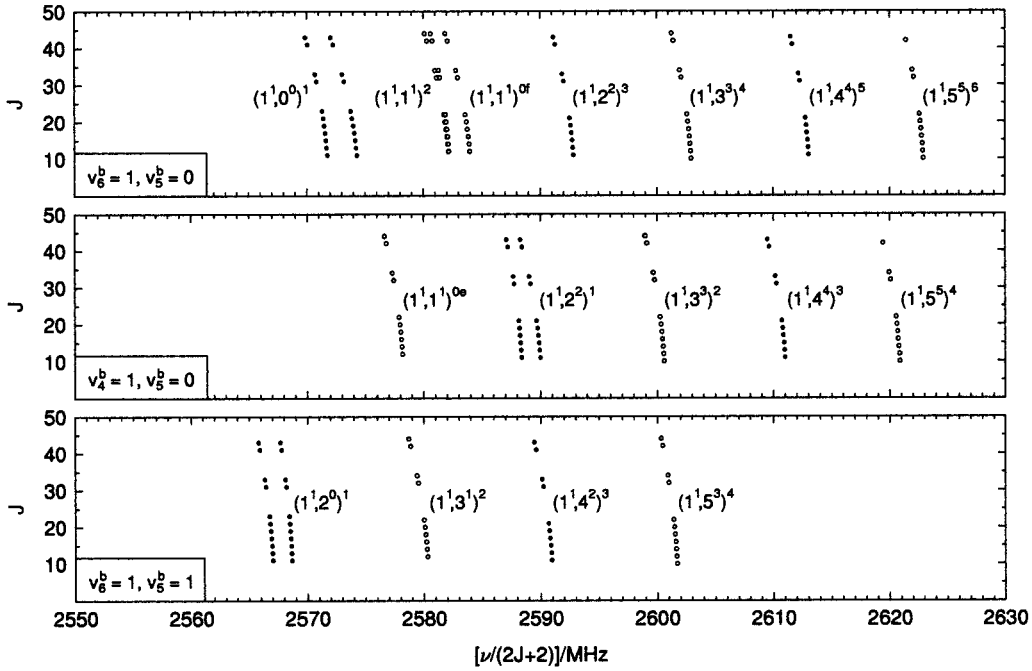


**Figure 6.** Fortrat diagram of rotational transitions of $^{35}$ClCNO in combination states of the CNO bending mode and the ClCN bending mode. Again, the series are labeled in terms of a linear molecule, i.e., $(v_4^{l_4}, v_5^{l_5})^k$, but arranged according to the nomenclature of a nearly prolate top molecule.

either to even higher excited states of the XCN bending mode or to states involving the CNO bending mode or the X−C stretching mode. In the case of BrCNO, presumably owing to strong global resonances, none of these series could be attributed to a specific vibrational state, but in the case of ClCNO, where accidental resonances appear to be less prevalent, a distinct pattern of related series could be identified, which was attributed to combination states of the CNO bending mode $\nu_4$ and the ClCN bending mode $\nu_5$, with $v_5 = 1-5$.

For each of these combination state series of ClCNO, the value of $k$ again was determined by examining the nuclear quadrupole splitting of the lowest observed rotational transitions, but neither the analysis of the nuclear quadrupole splitting nor the analysis of the observed $l$-type resonance splitting could provide a direct determination of the individual quantum numbers $l_4$ and $l_5$. Combining information from relative intensities and from a correlation diagram originally drawn by Yamada et al.[17] for the bending levels of fulminic acid HCNO and isocyanic acid HNCO, we nevertheless could obtain a tentative assignment, which is given in Table 1 and shown for $^{35}$ClCNO in Figure 6. Approximate term values based on relative intensities of the vibrational satellite lines for the lower bending levels are listed in Table 2.

**TABLE 2: Term Values for ($v_4$, $v_5$) = (1, $n$) Bending Levels of $^{35}$ClCNO, Derived from Relative Intensities of the Rotational Transitions**

| $(v_4^{l_4}, v_5^{l_5})^k$ | $(E/hc)$/cm$^{-1}$ | $(v_4^{l_4}, v_5^{l_5})^k$ | $(E/hc)$/cm$^{-1}$ |
|---|---|---|---|
| $(1^1, 1^1)^{0f}$ | 412[a] | | |
| $(1^1, 0^0)^1$ | 420 | $(1^1, 2^0)^1$ | 541 |
| $(1^1, 1^1)^2$ | 450 | $(1^1, 3^1)^2$ | 585 |
| $(1^1, 2^2)^3$ | 456 | $(1^1, 4^2)^3$ | 610 |
| $(1^1, 1^1)^{0e}$ | 450 | | |
| $(1^1, 2^2)^1$ | 447 | | 6 |

[a] Estimated error margins are 20 cm$^{-1}$.

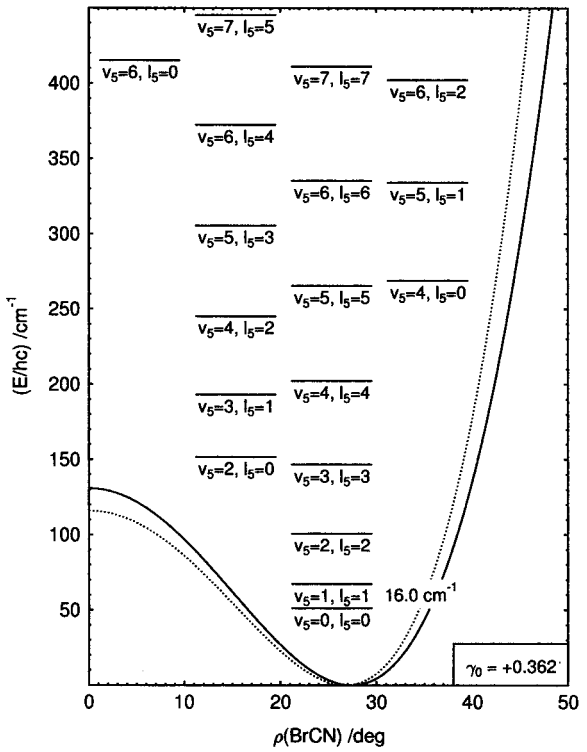


**Figure 7.** Effective bending potential from the GSRB analysis (solid curve) for the BrCN bending mode of BrCNO and resulting in BrCN bending levels. The bending levels are labeled in terms of a linear molecule with a two-dimensional BrCN bending mode. In terms of a nearly prolate top molecule, the different stacks correspond to the ground state, first excited state, and second excited state of a one-dimensional BrCN bending mode. The dotted curve represents the equilibrium bending potential calculated by Koput[9] at the CCSD(T)/cc-pV($Q$/5)Z level of theory. The bending coordinate $\rho$(BrCN) is defined as the supplement of the BrCN bond angle.

## Spectroscopic Constants

As already indicated in the previous section, nuclear quadrupole splitting of rotational transitions of BrCNO and ClCNO is dominated by the coupling of the respective halogen nuclei: Coupling constants for $^{79}$Br and $^{81}$Br nuclei are typically larger than 500 MHz, coupling constants for $^{35}$Cl and $^{37}$Cl nuclei are at least 50 MHz, whereas for the $^{14}$N nucleus in HCNO, Hüttner et al.[18] determined a coupling constant of only 245 kHz. For both BrCNO and ClCNO, in the investigated frequency range, the effect of nitrogen nuclear quadrupole coupling on the rotational transitions is more than an order of magnitude smaller than the experimental line width and therefore could be neglected. The same holds true for nuclear magnetic coupling.

For both isotopomers of both molecules, the halogen nucleus has a nuclear spin quantum number $I$ of $^3/_2$. Consequently, the total angular momentum quantum number $F$ of the rotating molecule in each case can take the values $J - {}^3/_2$, $J - {}^1/_2$, $J + {}^1/_2$, and $J + {}^3/_2$. Selection rules for rotational transitions of a linear molecule are $\Delta J = +1$ and $\Delta F = 0$ and $\pm 1$, but in the investigated frequency range, only the four $\Delta F = +1$ components were found to be of appreciable intensity. For $k = 0$, the $F = J - {}^3/_2$ component coincides with the $F = J - {}^1/_2$ component, whereas the $F = J + {}^3/_2$ component coincides with the $F = J + {}^1/_2$ component, and only a doublet is observed.

**TABLE 3: Results of the General SemiRigid Bender (GSRB) Analyses of the Rotational Transitions of BrCNO and ClCNO**

| | | BrCNO | ClCNO |
|---|---|---|---|
| $\rho_{min}$ | /rad | 0.478 74 (73) | 0.501 03 (73) |
| $f_{\alpha\alpha}$ | /aJrad$^{-2}$ | 0.081 16 (53) | 0.094 52 (60) |
| $c$ | /rad$^{-2}$ | −0.0438 (19) | −0.0508 (22) |
| $H$ | /cm$^{-1}$ | 130.82 (56) | 166.86 (84) |
| $r$(XC)$_{min}$ | /pm | 180.548 (25) | 165.249 (26) |
| $r$(CN)$_{min}$ | /pm | 117.32[a] | 117.47[a] |
| $r$(NO)$_{min}$ | /pm | 120.37[a] | 120.40[a] |
| $\alpha$(XCN)$_{min}$ | /deg | 152.570 (42)[b] | 151.293 (42)[b] |
| $\alpha$(CNO)$_{min}$ | /deg | 173.04[a] | 171.50[a] |
| $\phi$ | | 1.1530 (81) | 1.2067 (70) |
| $\partial^2 r$(XC)/$\partial\rho^2$ | /pmrad$^{-2}$ | 7.560 (61)[c] | 7.545 (53)[c] |
| $\partial^2 r$(CN)/$\partial\rho^2$ | /pmrad$^{-2}$ | 5.498 (45)[c] | 6.583 (46)[c] |
| $\partial^2 r$(NO)/$\partial\rho^2$ | /pmrad$^{-2}$ | −2.350 (19)[c] | −2.836 (20)[c] |
| $\sigma$ | /MHz | 1.332 | 3.029 |

[a] Taken from the ab initio calculations and held fixed. [b] Note that $\alpha$(XCN)$_{min}$/deg $\equiv 180 - (180\ \rho_{min}/\pi)$/rad. [c] Derived from the ab initio calculations and adjusted by fitting the scaling factor $\phi$.

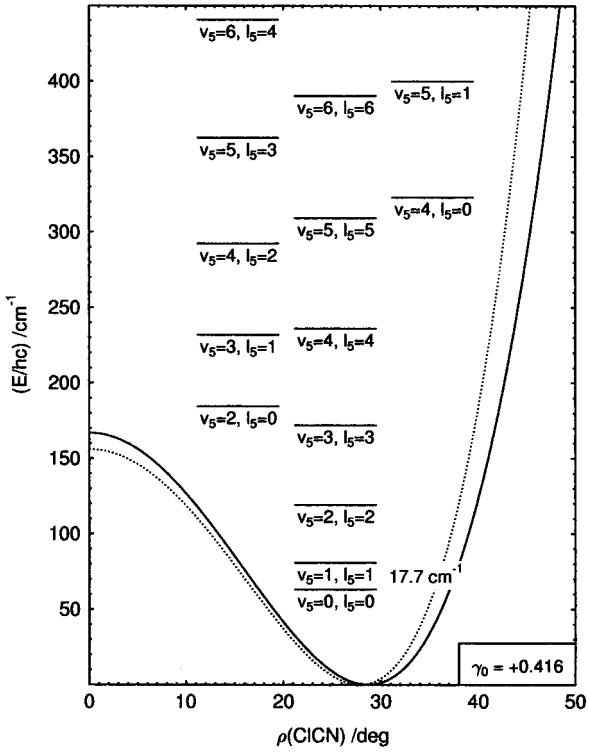


**Figure 8.** Effective bending potential from the GSRB analysis (solid curve) for the ClCN bending mode of ClCNO and resulting ClCN bending levels, labeled in terms of a linear molecule with a two-dimensional ClCN bending mode. In terms of a nearly prolate top molecule, the different stacks correspond to the ground state, first excited state, and second excited state of a one-dimensional ClCN bending mode. The dotted curve represents the equilibrium bending potential calculated by Koput[9] at the CCSD(T)/cc-pV($Q$/5)Z level of theory and corrected for relativistic effects. The bending coordinate $\rho$(ClCN) is defined as the supplement of the ClCN bond angle.

**TABLE 4: Term Values, Rotational Constants, and Centrifugal Distortion Constants for $v_5^{l_5}$ Bending Levels of $^{81}$BrCNO, Calculated from the GSRB Constants in Table 3[a]**

| | $G$/cm$^{-1}$ | $B_{ps}$/MHz[b] | | | | $D_{ps}$/Hz[b] | | | | |
|---|---|---|---|---|---|---|---|---|---|---|
| $v_5^{l_5 e/f}$ | $G$(srb) | $B_{ps}$(srb) | $\delta B_{ps}$ | $\Delta B_{ps}$(srb) | $\delta\Delta B_{ps}$ | $D_{ps}$(srb) | $\delta D_{ps}$ | $\Delta D_{ps}$(srb) | $\delta\Delta D_{ps}$ | $v_b$, $K_{a,l/u}$ |
| $0^{0e}$ | 0.0[c] | 1727.169 | −0.207 | 0.0 | 0.0 | 235 | 100 | 0 | 0 | 0, 0 |
| $1^{1e}$ | 16.0 | 1730.862 | 0.075 | 3.693 | 0.282 | 164 | 100 | −71 | 0 | 0, $1_l$ |
| $1^{1f}$ | 16.0 | 1736.462 | −0.083 | 9.293 | 0.124 | 202 | 100 | −33 | 0 | 0, $1_u$ |
| $2^{2e}$ | 49.6 | 1741.104 | 0.087 | 13.935 | 0.295 | 162 | 103 | −73 | 3 | 0, $2_l$ |
| $2^{2f}$ | 49.6 | 1741.104 | 0.083 | 13.935 | 0.290 | 158 | 100 | −77 | 0 | 0, $2_u$ |
| $3^{3e/f}$ | 95.5 | 1748.532 | 0.101 | 21.363 | 0.308 | 152 | 103 | −83 | 3 | 0, 3 |
| $4^{4e/f}$ | 150.9 | 1755.788 | 0.069 | 28.619 | 0.276 | 147 | 105 | −88 | 5 | 0, 4 |
| $5^{5e/f}$ | 214.0 | 1762.855 | 0.006 | 35.686 | 0.213 | 144 | 107 | −91 | 7 | 0, 5 |
| $6^{6e/f}$ | 283.9 | 1769.743 | −0.077 | 42.574 | 0.130 | 143 | 109 | −92 | 9 | 0, 6 |
| $7^{7e/f}$ | 359.5 | 1776.471 | −0.173 | 49.302 | 0.034 | 143 | 113 | −92 | 11 | 0, 7 |
| $8^{8e/f}$ | 440.4 | | | | | | | | | 0, 8 |
| $9^{9e/f}$ | 525.9 | | | | | | | | | 0, 9 |
| $2^{0e}$ | 100.4 | 1723.738 | −0.187 | −3.431 | 0.020 | 92 | 101 | −143 | 1 | 1, 0 |
| $3^{1e}$ | 141.9 | 1734.306 | 0.075 | 7.137 | 0.283 | 98 | 105 | −137 | 5 | 1, $1_l$ |
| $3^{1f}$ | 141.9 | 1740.380 | 0.018 | 13.211 | 0.225 | 123 | 107 | −112 | 6 | 1, $1_u$ |
| $4^{2e}$ | 193.8 | 1747.269 | 0.129 | 20.100 | 0.336 | 139 | 108 | −96 | 8 | 1, $2_l$ |
| $4^{2f}$ | 193.8 | 1747.269 | 0.128 | 20.100 | 0.335 | 116 | 107 | −119 | 7 | 1, $2_u$ |
| $5^{3e}$ | 253.9 | 1755.852 | 0.137 | 28.683 | 0.344 | 129 | 109 | −106 | 9 | 1, $3_l$ |
| $5^{3f}$ | 253.9 | 1755.852 | 0.138 | 28.683 | 0.345 | 129 | 110 | −106 | 10 | 1, $3_u$ |
| $6^{4e/f}$ | 320.8 | 1763.723 | 0.104 | 36.554 | 0.311 | 130 | 112 | −105 | 12 | 1, 4 |
| $7^{5e/f}$ | 393.7 | 1771.140 | 0.044 | 43.971 | 0.251 | 132 | 114 | −103 | 14 | 1, 5 |
| $8^{6e/f}$ | 471.9 | 1778.232 | −0.031 | 51.063 | 0.176 | 134 | 116 | −101 | 16 | 1, 6 |
| $9^{7e/f}$ | 554.8 | | | | | | | | | 1, 7 |
| $10^{8e/f}$ | 642.1 | | | | | | | | | 1, 8 |
| $4^{0e}$ | 217.4 | 1738.366 | −0.090 | 11.197 | 0.117 | 14 | 105 | −221 | 5 | 2, 0 |
| $5^{1e}$ | 282.6 | 1744.585 | −0.003 | 17.416 | 0.204 | 58 | 108 | −177 | 8 | 2, $1_l$ |
| $5^{1f}$ | 282.6 | 1751.915 | 0.012 | 24.746 | 0.219 | 76 | 110 | −159 | 10 | 2, $1_u$ |
| $6^{2e}$ | 350.7 | 1757.226 | 0.066 | 30.057 | 0.273 | 161 | 116 | −74 | 16 | 2, $2_l$ |
| $6^{2f}$ | 350.7 | 1757.225 | 0.066 | 30.056 | 0.274 | 84 | 112 | −151 | 12 | 2, $2_u$ |
| $7^{3e}$ | 423.2 | 1765.444 | 0.087 | 38.275 | 0.294 | 121 | 116 | −114 | 16 | 2, $3_l$ |
| $7^{3f}$ | 423.2 | 1765.444 | 0.086 | 38.275 | 0.294 | 121 | 116 | −114 | 16 | 2, $3_u$ |
| $8^{4e/f}$ | 500.3 | 1773.129 | 0.072 | 45.960 | 0.280 | 123 | 119 | −112 | 19 | 2, 4 |
| $9^{5e/f}$ | 581.8 | | | | | | | | | 2, 5 |
| $10^{6e/f}$ | 667.5 | | | | | | | | | 2, 6 |
| $6^{0e}$ | 363.5 | 1753.258 | −0.071 | 26.089 | 0.137 | −15 | 107 | −250 | 7 | 3, 0 |
| $7^{1e/f}$ | 441.9 | | | | | | | | | 3, 1 |
| $8^{2e}$ | 521.6 | 1768.470 | −0.084 | 41.301 | 0.123 | 234 | 138 | −1 | 38 | 3, $2_l$ |
| $8^{2f}$ | 521.6 | 1768.470 | −0.085 | 41.301 | 0.122 | 60 | 124 | −175 | 24 | 3, $2_u$ |
| $9^{3e}$ | 603.9 | | | | | | | | | 3, $3_l$ |
| $9^{3f}$ | 603.9 | | | | | | | | | 3, $3_u$ |
| $10^{4e/f}$ | 689.5 | | | | | | | | | 3, 4 |

[a] Derived quantities are defined in the text. [b] The column $\delta B_{ps}$ lists [$B_{ps}$(exp) − $B_{ps}$(srb)], and $\Delta B_{ps}$(srb) lists the calculated (GSRB) vibrational dependence of $B_{ps}$ given by [$B_{ps}(v_5^{l_5})$ − $B_{ps}(0^0)$](srb), whereas the difference between $\Delta B_{ps}$(exp) and $\Delta B_{ps}$(srb) is given in the next column, as $\delta\Delta B_{ps}$. The column headings for $D_{ps}$ are defined analogously. The experimental power series constants can be found in Table 1. [c] Ground-state term value with respect to the potential minimum is 51.1 cm$^{-1}$.

For a linear molecule, the frequencies of the $\Delta F = +1$ components of a rotational transition centered at $\nu_0$ are given by

$$\nu = \nu_0 + [E_Q(k, J+1, I, F+1) - E_Q(k, J, I, F)] \quad (3)$$

and the quadrupole energies $E_Q$ can be approximated by

$$E_Q = eQq\left[\frac{3k^2}{J(J+1)} - 1 \mp \delta_{k,1}\frac{\eta}{2}\right]\frac{3C(C+1) - 4I(I+1)J(J+1)}{8I(2I-1)(2J-1)(2J+3)}$$

$$C = F(F+1) - I(I+1) - J(J+1) \quad (4)$$

This equation is identical to the corresponding equation for *a*-type transitions of a nearly prolate top molecule, and hence must be applicable to quasilinear molecules as well.

Coupling constants $eQq$ for the various bending levels of BrCNO and ClCNO were determined by analysis of the lowest-frequency nonblended rotational transitions observed in the spectra. For BrCNO, the spectra recorded with a modulation deviation of 250 kHz usually provided a sufficient resolution except for $k = 1$ transitions, which had to be recorded again at a lower pressure and with a reduced modulation deviation. For ClCNO, the spectra recorded at Doppler-limited resolution were used. However, this resolution was not sufficient for a quantitative analysis of the $k = 1$ and 0 transitions, and therefore, the coupling constants were extrapolated from those determined for $k \geq 2$ within the same $v_5^b = n$ vibrational state (see Table 1 and Figure 5). A complete list of the nuclear quadrupole coupling constants for BrCNO and ClCNO can be found in Table 1. For $k = 1$, in addition to the coupling constant $eQq$, an asymmetry constant $\eta$ has to be considered. This constant, however, cannot be determined independently from $eQq$, and hence, the product $eQq\eta$ is reported. From the coupling and asymmetry constants

**TABLE 5: Term Values, Rotational Constants, and Centrifugal Distortion Constants for $v_5^{l_5}$ Bending Levels of $^{79}$BrCNO, Calculated from the GSRB Constants in Table 3[a]**

| | $G$/cm$^{-1}$ | $B_{ps}$/MHz[b] | | | | $D_{ps}$/Hz[b] | | | | |
|---|---|---|---|---|---|---|---|---|---|---|
| $v_5^{l_5 e/f}$ | $G$(srb) | $B_{ps}$(srb) | $\delta B_{ps}$ | $\Delta B_{ps}$(srb) | $\delta\Delta B_{ps}$ | $D_{ps}$(srb) | $\delta D_{ps}$ | $\Delta D_{ps}$(srb) | $\delta\Delta D_{ps}$ | $v_b$, $K_{a,l/u}$ |
| $0^{0e}$ | 0.0[c] | 1740.133 | −0.203 | 0.0 | 0.0 | 238 | 102 | 0 | 0 | 0, 0 |
| $1^{1e}$ | 16.0 | 1743.842 | 0.076 | 3.709 | 0.279 | 166 | 102 | −72 | 0 | 0, $1_l$ |
| $1^{1f}$ | 16.0 | 1749.521 | −0.084 | 9.388 | 0.119 | 205 | 102 | −33 | 0 | 0, $1_u$ |
| $2^{2e}$ | 49.6 | 1754.183 | 0.085 | 14.050 | 0.288 | 165 | 104 | −73 | 2 | 0, $2_l$ |
| $2^{2f}$ | 49.6 | 1754.183 | 0.081 | 14.050 | 0.284 | 160 | 102 | −78 | 0 | 0, $2_u$ |
| $3^{3e/f}$ | 95.5 | 1761.668 | 0.096 | 21.535 | 0.299 | 154 | 105 | −84 | 3 | 0, 3 |
| $4^{4e/f}$ | 151.0 | 1768.980 | 0.063 | 28.847 | 0.266 | 149 | 106 | −89 | 4 | 0, 4 |
| $5^{5e/f}$ | 214.2 | 1776.100 | −0.002 | 35.967 | 0.201 | 146 | 109 | −92 | 7 | 0, 5 |
| $6^{6e/f}$ | 284.1 | 1783.040 | −0.087 | 42.907 | 0.116 | 145 | 111 | −93 | 9 | 0, 6 |
| $7^{7e/f}$ | 359.5 | 1789.819 | −0.185 | 49.686 | 0.018 | 145 | 113 | −93 | 11 | 0, 7 |
| $8^{8e/f}$ | 440.8 | | | | | | | | | 0, 8 |
| $9^{9e/f}$ | 526.4 | | | | | | | | | 0, 9 |
| $2^{0e}$ | 100.5 | 1736.690 | −0.200 | −3.443 | 0.003 | 93 | 103 | −145 | 1 | 1, 0 |
| $3^{1e}$ | 142.0 | 1747.315 | 0.066 | 7.182 | 0.270 | 99 | 107 | −139 | 5 | 1, $1_l$ |
| $3^{1f}$ | 142.0 | 1753.474 | 0.010 | 13.341 | 0.213 | 125 | 107 | −113 | 5 | 1, $1_u$ |
| $4^{2e}$ | 194.0 | 1760.395 | 0.122 | 20.262 | 0.325 | 142 | 109 | −96 | 7 | 1, $2_l$ |
| $4^{2f}$ | 194.0 | 1760.395 | 0.122 | 20.262 | 0.325 | 118 | 109 | −120 | 7 | 1, $2_u$ |
| $5^{3e}$ | 254.2 | 1769.043 | 0.131 | 28.910 | 0.334 | 131 | 111 | −107 | 9 | 1, $3_l$ |
| $5^{3f}$ | 254.2 | 1769.043 | 0.131 | 28.910 | 0.334 | 131 | 111 | −107 | 9 | 1, $3_u$ |
| $6^{4e/f}$ | 321.2 | 1776.974 | 0.097 | 36.841 | 0.300 | 132 | 113 | −106 | 12 | 1, 4 |
| $7^{5e/f}$ | 394.2 | 1784.447 | 0.036 | 44.314 | 0.239 | 134 | 116 | −104 | 14 | 1, 5 |
| $8^{6e/f}$ | 472.4 | 1791.592 | −0.039 | 51.459 | 0.164 | 136 | 118 | −102 | 16 | 1, 6 |
| $9^{7e/f}$ | 555.4 | | | | | | | | | 1, 7 |
| $10^{8e/f}$ | 642.8 | | | | | | | | | 1, 8 |
| $4^{0e}$ | 217.6 | 1751.438 | −0.106 | 11.305 | 0.097 | 14 | 106 | −224 | 5 | 2, 0 |
| $5^{1e}$ | 282.9 | 1757.671 | −0.013 | 17.538 | 0.190 | 59 | 110 | −179 | 8 | 2, $1_l$ |
| $5^{1f}$ | 282.9 | 1765.106 | 0.001 | 24.973 | 0.204 | 77 | 112 | −161 | 10 | 2, $1_u$ |
| $6^{2e}$ | 351.1 | 1770.429 | 0.059 | 30.296 | 0.262 | 164 | 118 | −74 | 16 | 2, $2_l$ |
| $6^{2f}$ | 351.1 | 1770.429 | 0.058 | 30.296 | 0.261 | 85 | 113 | −153 | 11 | 2, $2_u$ |
| $7^{3e}$ | 423.7 | 1778.709 | 0.080 | 38.576 | 0.283 | 123 | 118 | −115 | 16 | 2, $3_l$ |
| $7^{3f}$ | 423.7 | 1778.709 | 0.080 | 38.576 | 0.283 | 123 | 118 | −115 | 16 | 2, $3_u$ |
| $8^{4e/f}$ | 501.0 | 1786.451 | 0.068 | 46.318 | 0.271 | 125 | 121 | −113 | 19 | 2, 4 |
| $9^{5e/f}$ | 582.6 | | | | | | | | | 2, 5 |
| $10^{6e/f}$ | 668.3 | | | | | | | | | 2, 6 |
| $6^{0e}$ | 364.0 | 1766.438 | −0.082 | 26.305 | 0.121 | −16 | 108 | −254 | 7 | 3, 0 |
| $7^{1e/f}$ | 442.4 | | | | | | | | | 3, 1 |
| $8^{2e}$ | 522.2 | 1781.760 | −0.078 | 41.627 | 0.125 | 239 | 139 | 1 | 37 | 3, $2_l$ |
| $8^{2f}$ | 522.2 | 1781.759 | −0.078 | 41.626 | 0.125 | 61 | 124 | −177 | 22 | 3, $2_u$ |
| $9^{3e/f}$ | 604.7 | | | | | | | | | 3, 3 |
| $10^{4e/f}$ | 690.4 | | | | | | | | | 3, 4 |

[a] Derived quantities are defined in the text. [b] The column $\delta B_{ps}$ lists [$B_{ps}$(exp) − $B_{ps}$(srb)], and $\Delta B_{ps}$(srg) lists the calculated (GSRB) vibrational dependence of $B_{ps}$ given by [$B_{ps}(v_5^{l_5})$ − $B_{ps}(0^0)$](srb), whereas the difference between $\Delta B_{ps}$(exp) and $\Delta B_{ps}$(srb) is given in the next column, as $\delta\Delta B_{ps}$. The column headings for $D_{ps}$ are defined analogously. The experimental power series constants can be found in Table 1. [c] Ground-state term value with respect to the potential minimum is 51.2 cm$^1$.

in Table 1 and the frequencies of the four $\Delta F = +1$ components, center frequencies were calculated for all visibly split rotational transitions. Together with the transition frequencies determined for transitions for which nuclear quadrupole splitting could not be resolved, these center frequencies are listed in the Supporting Information. The complete set of unsplit transition frequencies was then used to determine the final power series constants listed in Table 1.

### Semirigid Bender Analyses

To investigate quantitatively the internal dynamics of BrCNO and ClCNO, semirigid bender analyses of the rotational transitions in the vibrational ground state and in excited states of the XCN bending mode have been performed for each molecule with the General SemiRigid Bender (GSRB) program package,[4,5] utilizing the improved pseudo-potential-energy term $U(\rho)$ of Sarka and Bunker.[19] The semirigid bender model describes rotation-bending energy levels using a rigorous kinetic energy representation requiring only atomic masses, internuclear distances and bond angles, their dependence on the bending coordinate, and a model potential function. With the bending coordinate $\rho$ defined as the supplement of the bond angle α-(XCN), effective XCN bending potential functions $V(\rho)$ were chosen as

$$V(\rho) = \frac{H(1 + c\rho^2) f_{\alpha\alpha}(\rho^2 - \rho_{min}{}^2)^2}{f_{\alpha\alpha}\rho_{min}{}^4 + [8H(1 + c\rho^2) - f_{\alpha\alpha}\rho_{min}{}^2]\rho^2} \qquad (5)$$

The parameter $H$ adjusts the height of the Lorentzian barrier to linearity, and $f_{\alpha\alpha}$ is the harmonic force constant in the potential minimum at $\rho_{min}$. The anharmonicity in the vicinity of the potential minimum is adjusted by an additional parameter $c$, first introduced by Barrow et al.[20]

Initial values for the internuclear distances and bond angles at the potential minimum as well as for the dependence of the internuclear distances on the bending coordinate $\rho$ were taken from ab initio calculations at the CCSD(T)/cc-pVQZ level of theory, performed by Koput[9] during the course of the present investigation. These ab initio calculations yielded bent equilibrium geometries with angles $\alpha(XCN)_{min}$ of 154.80° for BrCNO and 152.18° for ClCNO.

**TABLE 6: Term Values, Rotational Constants, and Centrifugal Distortion Constants for $v_5^{l_5}$ Bending Levels of $^{37}$ClCNO, Calculated from the GSRB Constants in Table 3[a]**

| | $G$/cm$^{-1}$ | $B_{ps}$/MHz[b] | | | | $D_{ps}$/Hz[b] | | | | |
|---|---|---|---|---|---|---|---|---|---|---|
| $v_5^{l_5 e/f}$ | $G$(srb) | $B_{ps}$(srb) | $\delta B_{ps}$ | $\Delta B_{ps}$(srb) | $\delta\Delta B_{ps}$ | $D_{ps}$(srb) | $\delta D_{ps}$ | $\Delta D_{ps}$(srb) | $\delta\Delta D_{ps}$ | $v_b$, $K_{a,l/u}$ |
| $0^{0e}$ | 0.0[c] | 2511.752 | −0.306 | 0.0 | 0.0 | 398 | 185 | 0 | 0 | 0, 0 |
| $1^{1e}$ | 17.5 | 2514.735 | 0.234 | 2.983 | 0.540 | 265 | 188 | −133 | 2 | 0, $1_l$ |
| $1^{1f}$ | 17.5 | 2525.168 | −0.169 | 13.416 | 0.137 | 349 | 185 | −49 | −1 | 0, $1_u$ |
| $2^{2e}$ | 55.6 | 2529.801 | 0.177 | 18.049 | 0.483 | 272 | 187 | −126 | 2 | 0, $2_l$ |
| $2^{2f}$ | 55.6 | 2529.801 | 0.178 | 18.049 | 0.484 | 254 | 191 | −144 | 5 | 0, $2_u$ |
| $3^{3e/f}$ | 108.1 | 2539.766 | 0.196 | 28.014 | 0.502 | 251 | 192 | −147 | 6 | 0, 3 |
| $4^{4e/f}$ | 171.8 | 2549.560 | 0.130 | 37.808 | 0.436 | 244 | 194 | −154 | 9 | 0, 4 |
| $5^{5e/f}$ | 244.7 | 2559.125 | 0.012 | 47.373 | 0.318 | 240 | 197 | −158 | 12 | 0, 5 |
| $6^{6e/f}$ | 325.4 | 2568.463 | −0.142 | 56.711 | 0.164 | 238 | 201 | −160 | 16 | 0, 6 |
| $7^{7e/f}$ | 413.1 | 2577.590 | −0.316 | 65.838 | −0.011 | 237 | 207 | −161 | 22 | 0, 7 |
| $8^{8e/f}$ | 506.8 | | | | | | | | | 0, 8 |
| $9^{9e/f}$ | 606.1 | | | | | | | | | 0, 9 |
| $2^{0e}$ | 120.9 | 2504.744 | −0.518 | −7.008 | −0.212 | 165 | 189 | −233 | 4 | 1, 0 |
| $3^{1e}$ | 167.9 | 2518.018 | 0.106 | 6.266 | 0.412 | 156 | 196 | −242 | 11 | 1, $1_l$ |
| $3^{1f}$ | 167.9 | 2529.090 | −0.063 | 17.338 | 0.243 | 210 | 197 | −188 | 12 | 1, $1_u$ |
| $4^{2e}$ | 227.8 | 2537.188 | 0.249 | 25.436 | 0.555 | 245 | 201 | −153 | 16 | 1, $2_l$ |
| $4^{2f}$ | 227.8 | 2537.188 | 0.250 | 25.436 | 0.555 | 189 | 200 | −209 | 15 | 1, $2_u$ |
| $5^{3e/f}$ | 297.6 | 2548.932 | 0.325 | 37.180 | 0.631 | 216 | 204 | −182 | 19 | 1, 3 |
| $6^{4e/f}$ | 375.5 | 2559.679 | 0.303 | 47.927 | 0.609 | 217 | 208 | −181 | 23 | 1, 4 |
| $7^{5e/f}$ | 460.5 | 2569.792 | 0.211 | 58.040 | 0.517 | 219 | 213 | −179 | 28 | 1, 5 |
| $8^{6e/f}$ | 551.8 | 2579.449 | 0.069 | 67.697 | 0.375 | 222 | 217 | −176 | 32 | 1, 6 |
| $9^{7e/f}$ | 648.7 | 2588.758 | −0.111 | 77.006 | 0.195 | 224 | 223 | −174 | 38 | 1, 7 |
| $10^{8e/f}$ | 750.8 | | | | | | | | | 1, 8 |
| $11^{9e/f}$ | 857.6 | | | | | | | | | 1, 9 |
| $4^{0e}$ | 258.5 | 2523.870 | −0.114 | 12.118 | 0.192 | −5 | 195 | −403 | 10 | 2, 0 |
| $5^{1e}$ | 335.1 | 2531.187 | 0.085 | 19.435 | 0.391 | 79 | 201 | −319 | 15 | 2, $1_l$ |
| $5^{1f}$ | 335.1 | 2544.408 | 0.101 | 32.656 | 0.407 | 116 | 205 | −282 | 20 | 2, $1_u$ |
| $6^{2e}$ | 415.1 | 2550.212 | 0.224 | 38.460 | 0.530 | 314 | 221 | −84 | 36 | 2, $2_l$ |
| $6^{2f}$ | 415.1 | 2550.212 | 0.223 | 38.460 | 0.529 | 125 | 209 | −273 | 24 | 2, $2_u$ |
| $7^{3e}$ | 500.5 | 2561.498 | −0.121 | 49.746 | 0.185 | 207 | 151 | −191 | 34 | 2, $3_l$ |
| $7^{3f}$ | 500.5 | 2561.498 | −0.119 | 49.746 | 0.186 | 208 | 155 | −190 | 30 | 2, $3_u$ |
| $8^{4e/f}$ | 591.3 | 2572.011 | 0.357 | 60.259 | 0.663 | 211 | 222 | −187 | 37 | 2, 4 |
| $9^{5e/f}$ | 687.2 | 2581.962 | 0.279 | 70.210 | 0.585 | 214 | 228 | −184 | 43 | 2, 5 |
| $10^{6e/f}$ | 788.1 | 2591.486 | 0.223 | 79.734 | 0.529 | | | | | 2, 6 |
| $11^{7e/f}$ | 893.5 | | | | | | | | | 2, 7 |
| $6^{0e}$ | 432.0 | 2544.374 | 0.044 | 32.622 | 0.350 | −95 | 211 | −493 | 26 | 3, 0 |
| $7^{1e}$ | 525.3 | 2546.775 | −0.026 | 32.040 | −0.260 | 30 | 209 | −368 | 155 | 3, $1_l$ |
| $7^{1f}$ | 525.3 | 2562.553 | 0.153 | 37.385 | 0.322 | 67 | 219 | −331 | 84 | 3, $1_l$ |
| $8^{2e}$ | 620.1 | 2565.251 | −0.315 | 53.499 | −0.010 | 488 | 171 | 90 | −14 | 3, $2_l$ |
| $8^{2f}$ | 620.1 | 2565.251 | −0.318 | 53.499 | −0.012 | 73 | 135 | −325 | −50 | 3, $2_u$ |
| $9^{3e/f}$ | 717.9 | | | | | | | | | 3, 3 |
| $10^{4e/f}$ | 819.6 | | | | | | | | | 3, 4 |
| $11^{5e/f}$ | 925.0 | | | | | | | | | 3, 5 |

[a] Derived quantities are defined in the text. [b] The column $\delta B_{ps}$ lists [$B_{ps}$(exp) − $B_{ps}$(srb)], and $\Delta B_{ps}$(srb) lists the calculated (GSRB) vibrational dependence of $B_{ps}$ given by [$B_{ps}(v_5^{l_5})$ − $B_{ps}(0^0)$](srb), whereas the difference between $\Delta B_{ps}$(exp) and $\Delta B_{ps}$(srb) is given in the next column, as $\delta\Delta B_{ps}$. The column headings for $D_{ps}$ are defined analogously. The experimental power series constants can be found in Table 1. [c] Ground-state term value with respect to the potential minimum is 63.0 cm$^{-1}$.

The neglect in the semirigid bender model of those contributions to the centrifugal distortion which are due to the small amplitude modes would have led to significant systematic errors at high $J$. Therefore, the analyses have been confined to low-$J$ rotational transitions up to $J = 9 \leftarrow 8$. Because the rotational transitions below $J = 14$ for BrCNO and below $J = 10$ for ClCNO were not observed, extrapolated transition frequencies were calculated from the power series constants given in Table 1. In principle, one might think that a better extrapolation would be obtained from an effective Hamiltonian for a linear molecule or for an asymmetric top molecule, because a power series in integer powers of $J(J + 1)$ does not well reproduce $l$-type resonances or asymmetry doublings between closely spaced energy levels. However, both BrCNO and ClCNO are so far from the linear limiting case that efforts to analyze the data with an effective Hamiltonian for a linear molecule had to be abandoned, and the Watson Hamiltonian suitable for an asymmetric top molecule is equally inappropriate. As will be seen from the GSRB analyses, the spacings of the bending term values for both molecules are such that up to term values above 500 cm$^{-1}$ no bending levels that can interact strongly are closer than 13 cm$^{-1}$. Thus, the extrapolation with the power series constants is actually very reliable.

For each molecule, BrCNO and ClCNO, a simultaneous GSRB least-squares fit was performed for the two isotopomers. For both molecules, several trial runs were performed, to determine which parameters could be obtained from the pure rotational transitions. In the final analyses, the X−C internuclear distances were adjusted, whereas the C−N and N−O internuclear distances were held fixed at their ab initio values. The ab initio results for the variation of the internuclear distances with the bending coordinate $\rho$, $\partial^2 r/\partial\rho^2$, were scaled by fitting a common scaling factor $\phi$.

The results of the GSRB analyses are summarized in Table 3. The height of the barrier to linearity was determined to be 131 cm$^{-1}$ for BrCNO and 167 cm$^{-1}$ for ClCNO with XCN

**TABLE 7: Term Values, Rotational Constants, and Centrifugal Distortion Constants for $v_5^{l_5}$ Bending Levels of $^{35}$ClCNO, Calculated from the GSRB Constants in Table 3[a]**

| | $G$/cm$^{-1}$ | $B_{ps}$/MHz[b] | | | | $D_{ps}$/Hz[b] | | | | |
|---|---|---|---|---|---|---|---|---|---|---|
| $v_5^{l_5 e/f}$ | $G$(srb) | $B_{ps}$(srb) | $\delta B_{ps}$ | $\Delta B_{ps}$(srb) | $\delta\Delta B_{ps}$ | $D_{ps}$(srb) | $\delta D_{ps}$ | $\Delta D_{ps}$(srb) | $\delta\Delta D_{ps}$ | $v_b$, $K_{a,l/u}$ |
| $0^{0e}$ | 0.0[c] | 2573.094 | −0.312 | 0.0 | 0.0 | 416 | 194 | 0 | 0 | 0, 0 |
| $1^{1e}$ | 17.7 | 2576.083 | 0.214 | 2.989 | 0.527 | 276 | 196 | −140 | 2 | 0, $1_l$ |
| $1^{1f}$ | 17.7 | 2586.973 | −0.197 | 13.879 | 0.115 | 365 | 193 | −51 | −1 | 0, $1_u$ |
| $2^{2e}$ | 56.0 | 2591.628 | 0.142 | 18.534 | 0.454 | 283 | 196 | −133 | 2 | 0, $2_l$ |
| $2^{2f}$ | 56.0 | 2591.628 | 0.143 | 18.534 | 0.455 | 264 | 200 | −152 | 6 | 0, $2_u$ |
| $3^{3e/f}$ | 108.8 | 2601.839 | 0.149 | 28.745 | 0.462 | 262 | 200 | −154 | 6 | 0, 3 |
| $4^{4e/f}$ | 172.8 | 2611.870 | 0.074 | 38.776 | 0.386 | 255 | 203 | −161 | 9 | 0, 4 |
| $5^{5e/f}$ | 246.0 | 2621.664 | −0.055 | 48.570 | 0.258 | 251 | 206 | −165 | 12 | 0, 5 |
| $6^{6e/f}$ | 327.1 | 2631.225 | −0.219 | 58.131 | 0.093 | 249 | 210 | −167 | 16 | 0, 6 |
| $7^{7e/f}$ | 415.2 | 2640.569 | −0.404 | 67.475 | −0.092 | 248 | 216 | −168 | 22 | 0, 7 |
| $8^{8e/f}$ | 509.3 | | | | | | | | | 0, 8 |
| $9^{9e/f}$ | 609.0 | | | | | | | | | 0, 9 |
| $2^{0e}$ | 121.4 | 2566.011 | −0.599 | −7.083 | −0.287 | 170 | 199 | −246 | 5 | 1, 0 |
| $3^{1e}$ | 168.7 | 2579.475 | 0.041 | 6.381 | 0.353 | 162 | 205 | −254 | 11 | 1, $1_l$ |
| $3^{1f}$ | 168.7 | 2591.039 | −0.130 | 17.945 | 0.183 | 219 | 206 | −197 | 12 | 1, $1_u$ |
| $4^{2e}$ | 229.1 | 2599.210 | 0.190 | 26.116 | 0.502 | 258 | 210 | −158 | 16 | 1, $2_l$ |
| $4^{2f}$ | 229.1 | 2599.210 | 0.190 | 26.116 | 0.502 | 197 | 209 | −219 | 15 | 1, $2_u$ |
| $5^{3e/f}$ | 299.3 | 2611.231 | 0.266 | 38.137 | 0.578 | 226 | 214 | −190 | 20 | 1, 3 |
| $6^{4e/f}$ | 377.6 | 2622.232 | 0.241 | 49.138 | 0.553 | 227 | 219 | −189 | 25 | 1, 4 |
| $7^{5e/f}$ | 463.0 | 2632.582 | 0.144 | 59.488 | 0.456 | 229 | 223 | −187 | 29 | 1, 5 |
| $8^{6e/f}$ | 554.8 | 2642.467 | −0.007 | 69.373 | 0.305 | 232 | 228 | −184 | 34 | 1, 6 |
| $9^{7e/f}$ | 652.1 | 2651.995 | −0.199 | 78.901 | 0.113 | 234 | 235 | −182 | 41 | 1, 7 |
| $10^{8e/f}$ | 754.6 | | | | | | | | | 1, 8 |
| $11^{9e/f}$ | 862.0 | | | | | | | | | 1, 9 |
| $4^{0e}$ | 259.9 | 2585.656 | −0.214 | 12.562 | 0.098 | −8 | 204 | −424 | 10 | 2, 0 |
| $5^{1e}$ | 336.9 | 2592.960 | 0.003 | 19.866 | 0.315 | 80 | 211 | −336 | 17 | 2, $1_l$ |
| $5^{1f}$ | 336.9 | 2606.778 | 0.022 | 33.684 | 0.334 | 120 | 214 | −296 | 20 | 2, $1_u$ |
| $6^{2e}$ | 417.4 | 2612.559 | 0.141 | 39.465 | 0.453 | 335 | 232 | −81 | 38 | 2, $2_l$ |
| $6^{2f}$ | 417.4 | 2612.559 | 0.141 | 39.465 | 0.453 | 129 | 220 | −287 | 26 | 2, $2_u$ |
| $7^{3e}$ | 503.3 | 2624.103 | −0.041 | 51.009 | 0.271 | 218 | 192 | −198 | 2 | 2, $3_l$ |
| $7^{3f}$ | 503.3 | 2624.103 | −0.041 | 51.009 | 0.271 | 218 | 194 | −198 | 1 | 2, $3_u$ |
| $8^{4e/f}$ | 594.6 | 2634.858 | 0.288 | 61.764 | 0.600 | 221 | 232 | −195 | 38 | 2, 4 |
| $9^{5e/f}$ | 691.0 | 2645.041 | 0.196 | 71.947 | 0.508 | 224 | 240 | −192 | 47 | 2, 5 |
| $10^{6e/f}$ | 792.4 | 2654.786 | 0.122 | 81.692 | 0.434 | 228 | 249 | −188 | 55 | 2, 6 |
| $11^{7e/f}$ | 898.4 | 2664.181 | −0.092 | 91.087 | | | | | | 2, 7 |
| $6^{0e}$ | 434.4 | 2606.618 | −0.070 | 33.524 | 0.243 | −108 | 213 | −524 | 19 | 3, 0 |
| $7^{1e}$ | 528.2 | 2608.888 | −0.142 | 32.805 | −0.356 | 28 | 220 | −388 | 164 | 3, $1_l$ |
| $7^{1f}$ | 528.2 | 2625.379 | 0.040 | 38.406 | 0.237 | 67 | 233 | −349 | 91 | 3, $1_u$ |
| $8^{2e}$ | 623.5 | 2627.957 | −0.268 | 54.863 | 0.044 | 525 | 210 | 109 | 16 | 3, $2_l$ |
| $8^{2f}$ | 623.5 | 2627.956 | −0.269 | 54.862 | 0.043 | 74 | 168 | −342 | −26 | 3, $2_u$ |
| $9^{3e}$ | 722.0 | 2638.455 | 0.248 | | | 240 | 252 | −176 | 196 | 3, $3_l$ |
| $9^{3f}$ | 722.0 | 2638.455 | 0.247 | | | 228 | 264 | −188 | 122 | 3, $3_u$ |
| $10^{4e/f}$ | 824.2 | 2648.548 | −0.175 | | | | | | | 3, 4 |
| $11^{5e/f}$ | 930.2 | | | | | | | | | 3, 5 |

[a] Derived quantities are defined in the text. [b] The column $\delta B_{ps}$ lists [$B_{ps}$(exp) − $B_{ps}$(srb)], and $\Delta B_{ps}$(srb) lists the calculated (GSRB) vibrational dependence of $B_{ps}$ given by [$B_{ps}(v_5^{l_5})$ − $B_{ps}(0^0)$](srb), whereas the difference between $\Delta B_{ps}$(exp) and $\Delta B_{ps}$(srb) is given in the next column, as $\delta\Delta B_{ps}$. The column headings for $D_{ps}$ are defined analogously. The experimental power series constants can be found in Table 1. [c] Ground-state term value with respect to the potential minimum is 63.2 cm$^{-1}$.

angles of 152.57° and 151.29° at the potential minima. In accordance with the somewhat higher barrier to linearity, the harmonic force constant $f_{\alpha\alpha}$ for ClCNO was found to be about 15% larger than the force constant for BrCNO.

Graphic representations of the effective bending potentials with the resulting XCN bending levels are shown in Figures 7 and 8. It is the unusually structured manifold of these bending levels that explains the peculiar sequence of the observed rotational transition series. In terms of a linear molecule, the $l_5 = 0$ level of the second excited bending state indeed lies near the top of the barrier to linearity for both molecules. The grouping of the energy levels in Figures 7 and 8 corresponds to the notation for an asymmetric rotor, as employed in Figures 4 and 5, and highlights the truly quasilinear nature of both molecules. The calculated term values for each bending level, given in Tables 4 and 5 for the isotopomers of BrCNO and in Tables 6 and 7 for the isotopomers of ClCNO, are in satisfactory agreement with the relative intensities of the observed rotational transitions.

Tables 4−7 include a summary of the GSRB fits for each isotopomer of both molecules in terms of the power series constants $B_{ps}$(exp) and $B_{ps}$(srb) which were determined from the experimental and the semirigid bender (calculated with the constants of Table 3) rotational transition frequencies. The values of $B_{ps}$(exp) are given in Table 1, whereas in Tables 4−7, the values of $B_{ps}$(srb) and the direct residuals $\delta B_{ps} = B_{ps}$(exp) − $B_{ps}$(srb) are shown and similarly for $D_{ps}$. We have found it useful to also list $\Delta B_{ps}$(srb) = [$B_{ps}(v_5^{l_5})$ − $B_{ps}$(0°)](srb) and analogously $\Delta D_{ps}$(srb) in order to highlight the large amplitude bending contribution to $B_{ps}$ and $D_{ps}$. Finally, the residuals $\delta\Delta B_{ps} = \Delta B_{ps}$(exp) − $\Delta B_{ps}$(srb) and analogously $\delta\Delta D_{ps}$ show how well the GSRB Hamiltonian has reproduced the bending contribution to these two leading power series parameters.

If we look first at the values of $B_{ps}$, $\delta B_{ps}$, and $\Delta B_{ps}$, we see that for all four molecules the direct residuals $\delta B_{ps}$ are below 0.21 MHz but with a distinct trend within each asymmetric rotor grouping of term values and showing the largest errors for $K_a = l_5 = 0$. The residuals $\delta\Delta B_{ps}$ are gratifying, although they are all positive and roughly twice as large as the direct residuals. This trend, however, is easily understood from the relation $\delta\Delta B_{ps} = \delta B_{ps}(v_5^{l_5}) - \delta B_{ps}(0^\circ)$.

The values for $D_{ps}$, $\delta D_{ps}$, and $\Delta D_{ps}$ give a different picture. The direct residuals $\delta D_{ps}$ are all roughly half as large as the values of $D_{ps}$ themselves. This is one reason we explored the values of $\Delta D_{ps}$ and $\delta\Delta D_{ps}$, which confirm that the dependence of $D_{ps}$ on bending excitation is actually well reproduced by the GSRB calculation. The large, nearly constant offsets expressed by the residuals $\delta D_{ps}$ suggest that the omitted contributions of the small amplitude modes to the centrifugal distortion constant $D_{ps}$ actually are substantial. The small $\delta\Delta D_{ps}$ values also show a positive trend, corresponding to a negative trend in terms of the rotational energy. The information contained in Tables 4−7 allows us to separate, at least roughly, the limitations because of this particular lack in the theoretical model ($\delta D_{ps}$) from those presumably because of the simplified representation of the bending potential in the Hamiltonian ($\delta\Delta D_{ps}$ and $\delta\Delta B_{ps}$).

The $\Delta D_{ps}$ values in Tables 4−7 for all four molecules indicate that those energy levels most affected by interactions are $l_5 = 2$ and 0 levels for $v_5 \geq 4$ or $v_5^b \geq 1$; at higher excitation, the barrier to linearity loses its influence on the energy level spacing and the pattern becomes more that of a linear molecule (see Figures 7 and 8).

## Discussion

From the spacing of the term values shown in Figures 7 and 8 and given in Tables 4−7, quasilinearity parameters $\gamma_0$ as defined by Yamada and Winnewisser[2] can be calculated to be +0.362 for BrCNO and +0.416 for ClCNO. These numbers indicate that both molecules are more bent than OCCCO, which has $\gamma_0 = -0.203$,[14] yet still more linear than HNCS with $\gamma_0 = +0.688$ or $CH_2(^3B_1)$ with $\gamma_0 = +0.697$.[21,22] The only other chain molecule for which similar internal dynamics have been deduced, though never explicitly verified, is HNCSe with an estimated quasilinearity parameter $\gamma_0$ of +0.460.[23] Comparable bending dynamics, however, were reported for two quasisymmetric top molecules, $SiH_3OSiH_3$ and $CH_3NCS$.[24,25]

In terms of a nearly prolate top molecule, XCN fundamental transition wavenumbers are 100.5 $cm^{-1}$ for BrCNO and 121.4 $cm^{-1}$ for ClCNO. In terms of a linear molecule, however, the XCN fundamental transition wavenumbers are only 16.0 and 17.7 $cm^{-1}$. The CCC fundamental transition wavenumber of OCCCO, for comparison, lies at 18.2 $cm^{-1}$.[26] A search for the low-lying bending fundamental of BrCNO in the submillimeter-wave region with the Cologne terahertz spectrometer[27] was not successful, probably due to a very small transition moment for these transitions, which are *b*-type transitions in the notation of a prolate asymmetric top molecule. However, some high-*J* *a*-type transitions were observed for both bromine isotopomers of BrCNO. Because of their relatively large experimental errors, these transitions were not included in the current data set.

From a chemical point of view, it is remarkable that BrCNO and ClCNO are much closer to the bent limiting case than HCNO, which with a quasilinearity parameter $\gamma_0$ of −0.657 is still a fairly linear molecule.[28] The fundamental difference becomes even more obvious in terms of the XCN bending potentials: Whereas for BrCNO and ClCNO we have determined barrier heights of 131 and 167 $cm^{-1}$, for the parent molecule HCNO, an effective barrier height of only 12 $cm^{-1}$ was found.[29] On the basis of preliminary results from medium-level ab initio calculations, we believe that the different effective bending potentials essentially reflect the $\pi$-electron donor properties of the halogen atoms.

It is important to keep in mind that effective bending potentials derived from semirigid bender analyses cannot be strictly identified with equilibrium bending potentials, because the former incorporate zero-point contributions to the bending potential due to the small-amplitude vibrations. These contributions have been quantified in the case of HCNO and OCCCO, where effective bending potentials could be determined for excited states of the small-amplitude vibrations as well.[29] However, in the case of BrCNO and ClCNO, the experimental data required for that purpose are not yet available. Nevertheless, it seems likely that the effective barrier heights determined in the present investigation are no more than 10−30 $cm^{-1}$ higher than the equilibrium values.

At the CCSD(T)/cc-pVQZ level of theory, Koput[9] has calculated equilibrium barriers to linearity to be 95 $cm^{-1}$ for BrCNO and 159 $cm^{-1}$ for ClCNO. Using the cc-pV5Z basis set for the halogen atoms, barrier heights of 100 and 156 $cm^{-1}$ were found, and the additional inclusion of relativistic corrections for the bromine nucleus in BrCNO brought its barrier height up to 119 $cm^{-1}$. These results are in excellent agreement with our experimental findings. It is thus fair to say that the CCSD(T) method in conjunction with sufficiently large one-particle basis sets was as successful in predicting the equilibrium XCN bending potentials of BrCNO and ClCNO as it had been previously in reproducing both the equilibrium HCN bending potential of HCNO and the equilibrium CCC bending potential of OCCCO.[30]

**Acknowledgment.** We are grateful to N.P.C. Westwood for many valuable comments and for his assistance with the syntheses, and we are indebted to J. Koput for stimulating discussions and for providing the results of his studies prior to publication. This work was supported in part by the Deutscher Akademischer Austauschdienst, by the Fonds der Chemischen Industrie, by the Alexander von Humboldt Foundation, by the Deutsche Forschungsgemeinschaft, and by the Natural Sciences and Engineering Research Council of Canada.

**Supporting Information Available:** Tables including all assigned and analyzed experimental transition frequencies for BrCNO and ClCNO as well as all extrapolated transition frequencies used as basis for the semirigid bender analyses. This material is available free of charge via the Internet at http://pubs.acs.org.

## References and Notes

(1) Thorson, W. R.; Nakagawa, I. *J. Chem. Phys.* **1960**, *33*, 994.
(2) Yamada, K.; Winnewisser, M. *Z. Naturforsch. A* **1976**, *31*, 139.
(3) Winnewisser, B. P. In *Molecular Spectroscopy: Modern Research*; Narahari Rao, K., Ed.; Academic Press: Orlando, FL, 1985; Vol. III.
(4) Ross, S. C. *J. Mol. Spectrosc.* **1988**, *132*, 48.
(5) Ross, S. C.; Cooper, T. A.; Firth, S.; Kroto, H. W.; Walton, D. R. M. *J. Mol. Spectrosc.* **1992**, *152*, 152.
(6) Pasinszki, T.; Westwood, N. P. C. *J. Phys. Chem.* **1995**, *99*, 6401.
(7) Pasinszki, T.; Westwood, N. P. C. *J. Phys. Chem. A* **1998**, *102*, 4939.
(8) Gillies, C. W.; Gillies, J. Z.; Lichau, H.; Winnewisser, B. P.; Winnewisser, M. *Chem. Phys. Lett.* **1998**, *285*, 391.
(9) Koput, J. *J. Phys. Chem. A* **1999**, *103*, 2170. *J. Phys. Chem. A* **1999**, *103*, 6017.
(10) Winnewisser, M.; Lichau, H.; Wolf, F. *J. Mol. Spectrosc.* **2000**, *202*, 155.

(11) Maiwald, F.; Lewen, F.; Vowinkel, B.; Jabs, W.; Paveljev, D. G.; Winnewisser, M.; Winnewisser, G. *IEEE Microwave Guided Wave Lett.* **1999**, *9*, 198.
(12) Savitzky, A.; Golay, M. J. E. *Anal. Chem.* **1964**, *36*, 1627.
(13) Preu$\beta$er, J. Ph.D. Dissertation, Justus-Liebig-Universität: Gie$\beta$en, Germany, 1994.
(14) Vander Auwera, J.; Johns, J. W. C.; Polyansky, O. L. *J. Chem. Phys.* **1991**, *95*, 2299.
(15) King, M. A.; Kroto, H. W.; Landsberg, B. M. *J. Mol. Spectrosc.* **1985**, *113*, 1.
(16) Yamada, K.; Winnewisser, M.; Winnewisser, G.; Szalanski, L. B.; Gerry, M. C. L. *J. Mol. Spectrosc.* **1977**, *64*, 401. Yamada, K.; Winnewisser, M. *J. Mol. Spectrosc.* **1978**, *72*, 484.
(17) Yamada, K.; Winnewisser, B. P.; Winnewisser, M. *J. Mol. Spectrosc.* **1975**, *56*, 449. Because the correct assigment was not yet known, the $v_4^b = 1$ levels were drawn at the term values of the $v_6^b = 1$ levels and vice versa.
(18) Hüttner, W.; Bodenseh, H. K.; Nowicki, P.; Morgenstern, K. *J. Mol. Spectrosc.* **1978**, *71*, 246.
(19) Sarka, K.; Bunker, P. R. *J. Mol. Spectrosc.* **1987**, *122*, 259.
(20) Barrow, T.; Dixon, R. N.; Duxbury, G. *Mol. Phys.* **1974**, *27*, 1217.
(21) Ross, S. C.; Niedenhoff, M.; Yamada, K. M. T. *J. Mol. Spectrosc.* **1994**, *164*, 432. Niedenhoff, M.; Winnewisser, G.; Yamada, K. M. T.; Belov, S. P. *J. Mol. Spectrosc.* **1995**, *169*, 224. Niedenhoff, M.; Yamada, K. M. T.; Winnewisser, G. *J. Mol. Spectrosc.* **1997**, *183*, 176.
(22) Sears, T. J.; Bunker, P. R.; McKellar, A. R. W.; Evenson, K. M.; Jennings, D. A.; Brown, J. M. *J. Chem. Phys.* **1982**, *77*, 5348. Sears, T. J.; Bunker, P. R.; McKellar, A. R. W. *J. Chem. Phys.* **1982**, *77*, 5363.
(23) Vogt, J.; Winnewisser, M. *Ber. Bunsen-Ges. Phys. Chem.* **1984**, *88*, 439. Vogt, J.; Winnewisser, M. *Ber. Bunsen-Ges. Phys. Chem.* **1984**, *88*, 444.
(24) Durig, J. R.; Flanagan, M. J.; Kalasinsky, V. F. *J. Chem. Phys.* **1977**, *66*, 2775. Koput, J.; Wierzbicki, A. *J. Mol. Spectrosc.* **1983**, *99*, 116.
(25) Koput, J. *J. Mol. Spectrosc.* **1986**, *118*, 189.
(26) Burenin, A. V.; Karyakin, E. N.; Krupnov, A. F.; Shapin, S. M. *J. Mol. Spectrosc.* **1979**, *78*, 181. Karyakin, E. N.; Krupnov, A. F.; Shapin, S. M. *J. Mol. Spectrosc.* **1982**, *94*, 283.
(27) Winnewisser, G.; Krupnov, A. F.; Tretyakov, M. Y.; Liedtke, M.; Lewen, F.; Saleck, A. A.; Schieder, R.; Shkaev, A. P.; Volokhov, S. V. *J. Mol. Spectrosc.* **1994**, *165*, 294.
(28) Winnewisser, B. P.; Winnewisser, M.; Winther, F. *J. Mol. Spectrosc.* **1974**, *51*, 65.
(29) Bunker, P. R.; Landsberg, B. M.; Winnewisser, B. P. *J. Mol. Spectrosc.* **1979**, *74*, 9. Jensen, P. *J. Mol. Spectrosc.* **1983**, *101*, 422.
(30) Koput, J.; Winnewisser, B. P.; Winnewisser, M. *Chem. Phys. Lett.* **1996**, *255*, 357. Koput, J. *Chem. Phys. Lett.* **2000**, *320*, 237.